

INVESTIGATION OF THE FEASIBILITY OF USING CHIRP-EVOKED ABR IN
ESTIMATION OF LOUDNESS GROWTH

M.Sc. Thesis – S. Hoseingholizade; McMaster University – Psychology, Neuroscience and Behaviour.

INVESTIGATION OF THE FEASIBILITY OF USING CHIRP-EVOKED ABR IN
ESTIMATION OF LOUDNESS GROWTH

By SIMA HOSEINGHOLIZADE, M.SC.

A Thesis Submitted to the School of Graduate Studies in Partial Fulfilment of
the Requirements for the Degree Master of Science

McMaster University © Copyright by Sima Hoseingholizade, September 2015

M.Sc. Thesis – S. Hoseingholizade; McMaster University – Psychology, Neuroscience and Behaviour.

MASTER OF SCIENCE (2015)

McMaster University

Psychology, Neuroscience, and Behaviour

TITLE: Investigation of the feasibility of using chirp-evoked ABR in estimation of loudness growth

AUTHOR: Sima Hoseingholizade, M.Sc.

SUPERVISOR: Dr. Laurel J. Trainor

Abstract:

Loudness growth evaluation is important to comprehend the theoretical implication of loudness in both normal hearing and hearing impaired people, as well as applied applications in hearing-aid design. However, current psychoacoustic procedures are subjective, time consuming and require the constant attention of participants. The primary aim of the present study is to investigate the feasibility of objectively assessing the loudness growth function by using the Auditory Brainstem Response (ABR). Previous studies applied either non-frequency specific click stimuli or tone burst stimuli to evoke auditory brainstem responses. Although the advantage of a chirp stimulus in producing a more reliable response has been well documented in many studies, no one has previously used this stimulus to evaluate loudness growth functions. One octave-band chirp stimuli with center frequencies of 1000 Hz and 4000 Hz were chosen to evoke ABRs at 7 different stimulus intensities from 20 dB nHL to 80 dB nHL with 10 dB steps. In the psychoacoustic procedure, subjects were asked to rate the perceived loudness of each presented stimulus. The recorded ABR trials were averaged by a modified version of weighted averaging based on Bayesian inference. This method of averaging decreases the effects of non-stationary noise sources by calculating a number of locally-stationary noise sources based on a series of F-tests. The peak-to-trough amplitude of the most salient peak of the ABR at each intensity constituted the physiological loudness estimate. Linear and power functions relating the psychoacoustical results and the ABR measurements were compared. The obtained results were in good agreement with equal-loudness contours and estimated loudness from the loudness model for time-varying sounds of Glasberg, & Moore (2002). We concluded that loudness growth can be estimated with ABRs to frequency-specific chirp stimuli.

Acknowledgments

I would never have been able to finish my dissertation without the guidance of my committee members, help from friends, and support from my family and spouse.

Firstly, I would like to express my sincere gratitude to my advisor Prof. Laurel Trainor for the continuous support of my M.Sc. study and related research, for her patience, motivation, and immense knowledge. Her guidance helped me in all the time of research and writing of this thesis. I could not have imagined having a better advisor and mentor for my M.Sc. study.

My sincere thanks also goes to Dr. Ian Bruce and Dr. Sue Becker, who provided me with their insightful comments, excellent guidance and also their help in editing this manuscript.

I thank my fellow labmates specifically Ranya Amirthamanoharan for helping me collect ABR samples.

Last but not the least, I would like to thank my family without which none of this would have been possible. To my spouse and my son thank you for supporting me spiritually throughout writing this thesis and my life in general.

Table of Contents

1. Introduction.....	1
1.1 General Auditory Anatomy and Physiology.....	2
1.1.1 Outer ear and middle ear.....	2
1.1.2 Cochlea (inner ear).....	3
1.1.2.1 Cochlea Amplifier.....	6
1.2 Loudness Growth.....	7
1.2.1 Loudness Growth Models for Normal Listeners.....	9
1.2.2 Psychoacoustical Procedures for Estimating Loudness Growth.....	10
1.3 Auditory Brainstem Response.....	11
1.3.1 ABR Stimuli.....	13
1.3.1.1 Chirp Stimuli.....	16
1.3.2 ABR Signal Processing.....	21
1.4. Previous studies of using ABR to evaluate loudness growth.....	25
2. Methodology and experiments.....	30
2.1 Subjects.....	30
2.2 General Procedure.....	30
2.3 Stimuli and Calibration.....	30
2.4 Psychoacoustic Experiment.....	35
2.5 Recording Paradigm of the ABR experiment.....	36

2.6 Estimation of Loudness Growth from Evoked ABRs and Psychoacoustic Procedure.....	37
3. Results.....	39
3.1 Psychoacoustical Results	39
3.2 Chirp Evoked ABR Results	42
3.3 Estimation of Individual Loudness Growth through Evoked ABR	44
3.3.1 Linear Function Fitting	45
3.3.2 Fitting Power function	48
3.3.3 Comparison between Linear and Power Function Fitting	50
4. Discussion.....	53
5. Summary and Conclusion.....	61
Reference	63
Appendix	70

List of Figures

Chapter 1	1
Figure 1-1: a general schematic overview of the peripheral auditory system (Schnupp, Nelken, & King, 2010).	3
Figure 1-2: Cross-section of the cochlea (Schnupp et al., 2011).	4
Figure 1-3: The membrane does not move as a unit; instead, successive waves propagate from the base of the cochlea towards its apex (Hudspeth, 2014).	5
Figure 1-4: Excitation pattern of basilar membrane to a 10 KHz stimulus. It is clear that at lower levels, frequency tuning is sharper while at higher levels, it is more broadly tuned (Ruggero & Rich, 1991).	6
Figure 1-5: Frequency spectra of BM responses to 75-dB SPL clicks in chinchilla before (solid line) and after (dashed line) the intravenous injection of furosemide. It is obvious that after injection, frequency tuning is reduced and basilar membrane response to stimulus is linear (Robles & Ruggero, 2001).	7
Figure 1-6: Equal loudness counters (Hamill & Price, 2008).	8
Figure 1-7: Comparing three loudness growth functions.....	10
Figure 1-8: A schematic of the auditory evoked potential signal in human. The ABR response is up to approximately 20 ms, the MLR is between 20 and 40 ms, and the LLR is between 50 to 100 ms after stimulus onset (Melcher, 2009).	12
Figure 1-9: Recorded ABR waveform (Burkard, Eggermont, & Don, 2007).....	13
Figure 1-10: The tonotopic map along the basilar membrane.	14

Figure 1-11: Time-Frequency representation on the basilar membrane of the click ABR for the first 4 ms. It is obvious that each frequency component of the click stimuli is separated in time as the result of temporal dispersion (Kiang, 1975) 15

Figure 1-12: Narrow frequency bands ABRs (left) are shifted summed to construct the Stacked ABR (right) (Don, 2002). 17

Figure 1-13: Chirp (left) and click (right) stimulus (Jill, 2010). 18

Figure 1-14: Four different cochlea delay models extracted from narrow-band ACAP of (Eggermont, 1979), tone-burst ABR of (Neely et al., 1988), narrow-band ABR of (Don, Kwong, & Tanaka, 2005) and a cochlear model of (de Boer, 1980) (Elberling et al., 2007).. 19

Figure 1-15: Comparison between different methods of averaging on a data with a sudden increasing amount of noise (Don & Elberling, 1994). 23

Chapter 2 30

Figure 2-1: Amplitude-frequency characteristics of the filters applied for constructing CE-chirp stimuli and the four octave band chirps with four center frequencies of 500, 1000, 2000 and 4000 Hz (Elberling & Don, 2010) Only those with center frequencies of 1000 and 4000 Hz were used in the present study. 31

Figure 2-2: One octave-band chirp stimulus with center frequency of 1000 Hz. 32

Figure 2-3: One octave-band chirp stimulus with center frequency of 4000 Hz. 32

Figure 2-4: Defining the peak-to-peak equivalent Reference Equivalent Threshold Sound Pressure Levels (peRETSPLs). The dB peSPL of each octave-band chirp is equal the sound pressure level (dB SPL) of the sinusoidal signal whose frequency corresponds to the center frequency of the octave-band chirp (Gøtsche-Rasmussen et al., 2012) 34

Figure 2-5: A schematic view of measuring the peak-to-peak equivalent Reference Equivalent Threshold Sound Pressure Levels (peRETSPLs) (Fedtke & Hensel, 2010). 34

Figure 2-6: The behavioral instruction given to each participant to help them to do the task. . 36

Chapter 3..... 39

Figure 3-1: The normative reference (i.e., categories versus sound level (dB nHL)) for data from seven published loudness scaling procedures and the present study. Each category unit shows a specific loudness scale (i.e., 0 assigned to ‘not heard’, 1 assigned to ‘very soft’, 2 assigned to ‘soft’, 3 assigned to ‘OK-comfortable’, 4 assigned to ‘loud’, 5 assigned to ‘very loud’ and 6 assigned to ‘too loud’). 42

Figure 3-2: The averaged wave V amplitude data (across subjects) and standard deviation as a function of stimuli intensity (dB nHL). The left plot corresponds to obtained data from evoked ABRs to one-octave band chirp stimulus with center frequency of 1000 Hz and the right plot shows that of evoked ABRs to one-octave band chirp stimulus with center frequency of 4000 Hz. 44

Figure 3-3: Linear fitting using data of all the participants with one octave-band chirp stimulus with 1000 Hz center frequency. 47

Figure 3-4: Linear function fitting using data of all the participants with one octave-band chirp stimulus with 4000 Hz center frequency. 47

Figure 3-5: Power-law function fitting using data from all participants with the one octave-band chirp stimulus with 1000 Hz center frequency. 49

Figure 3-6: Power-law function fitting using data from all the participants with the one octave-band chirp stimulus with 4000 Hz center frequency. 50

Chapter 4..... 53

Figure 4-1 Relationship between R-Squared values (linear fit between psychoacoustic data and wave V amplitude) for each subject at 1000 and 4000 Hz..... 54

Figure 4-2: Comparison between psychoacoustic and ABR data for the two individuals with the worst (upper plot) and the best (lower plot) linear fit for the 1000 Hz chirp stimulus. 54

Figure 4-3: Comparison between psychoacoustic and ABR data for the two individuals with the worst (upper plot) and the best (lower plot) linear fit for the 4000 Hz chirp stimulus. 55

Figure 4-4: Estimated loudness scale at each amplitude of wave V for linear obtained models. The blue line is relative to the obtained linear models for the 1000 Hz chirp stimulus. The red line shows the linear model obtained for the 4000 Hz chirp stimulus. 57

Figure 4-5: The relationship of loudness in phons to intensity level (in decibels) for normal hearing people. The curved lines are equal-loudness curves (Metabolic, 2012). 58

Figure 4-6: Estimated loudness (phon) based on the model of Glasberg, & Moore (2002) for two different stimuli presented at the same intensity levels (dB nHL). 60

Figure 4-7: Linear function fitted on the obtained loudness scales from the psychoacoustic tasks as a function of stimulus level (in dB nHL). The blue line is relative to the obtained linear fit for the 4000 Hz chirp stimulus. The red line shows the linear fit obtained for the 1000 Hz chirp stimulus. 60

List of Tables

Chapter 2	30
Table 2-1: Reference threshold values in dB peETSPL for one octave-band chirps at the repetition rate 20 stimuli/s, using 2cc-coupler presented in the ER-3A (personal communication with Dr. Elberling, 2015).	33
Chapter 3	39
Table 3-1: The normative reference data corresponding to the common categories very soft, soft, comfortable, loud, very loud, and too loud from one-octave band chirp stimuli (this study) and the seven procedures presented in (Elberling, 1999) in dB HL.	40
Table 3-2: Stimulus type in each loudness scaling psychoacoustic task.....	41
Table 3-3: Power-law exponent of the curve-fitting for each psychoacoustic method.....	42
Table 3- 4: Average and standard deviations of measured amplitude of wave V across all the participants. Evoked ABR was obtained by presenting the one octave-band chirp stimulus with 1000 Hz center frequency.	43
Table 3-5: Average and standard deviations of measured amplitude (microvolt) of wave V across all the participants. Evoked ABR was obtained by presenting the one octave-band chirp stimulus with 4000 Hz center frequency.	43
Table 3-6: R-squared values for linear fitting between psychoacoustic and ABR estimates of loudness growth for each individual participant with one octave-band chirp stimulus with center frequency of 1000 Hz. The first column shows the ordinary fitting and second column shows the linear weighted fitting.	46

Table 3-7: R-squared values for linear fitting between psychoacoustic and ABR estimates of loudness growth for each individual participant with one octave-band chirp stimulus with center frequency of 4000 Hz. The first column shows the ordinary fitting and second column shows the linear weighted fitting. 46

Table 3-8: R-squared values for the power function fitting between psychoacoustic and ABR estimates of loudness growth for each individual participant with the one octave-band chirp stimulus with center frequency of 1000 Hz. The first column shows the ordinary fitting and the second column shows the power function weighted fitting. 48

Table 3-9: R-squared for power function fitting between psychoacoustic and ABR estimates of loudness growth for each individual participant for the one octave-band chirp stimulus with center frequency of 4000 Hz. The first column shows the ordinary fitting and the second column shows the power function weighted fitting. 49

Table 3-10: Adjusted R-squared values for each individual for the two weighted fitting functions, linear and power for the one octave-band chirp stimulus with center frequency of 1000 Hz. 51

Table 3-11: Adjusted R-squared values for each individual for the two weighted fitting functions, linear and power for the one octave-band chirp stimulus with center frequency of 4000 Hz. 52

Chapter1: Introduction

The main goal of the present thesis is to establish an objective procedure for the estimation of individual loudness growth functions by measuring evoked Auditory Brainstem Responses (ABRs) to one octave-band chirp stimuli. At present, brainstem responses are typically only used in clinical settings to measure thresholds in populations such as infants who are unable to communicate through speech. However, an objective procedure for loudness growth estimation would be useful for populations that are not capable in performing psychoacoustical tasks, such as infants and cognitively impaired patients.

It is well documented that loudness growth varies considerably among both normal-hearing and hearing-impaired individuals. For example, loudness growth functions can be extremely different among hearing-impaired listeners with similar thresholds (Buus & Florentine, 2001). Thus, finding an accurate objective way to estimate loudness growth would provide a better understanding of loudness growth, as well as have applications to nonlinear hearing aid fitting.

The idea of finding an objective approach for loudness growth estimation is not a new one, and several studies have attempted to find correlations between loudness and specific features of recorded ABRs (e.g. Pratt & Sohmer, 1977; Wilson & Stelmack, 1982; S. A. Davidson, Wall, & Goodman, 1990; Thornton, Yardley, & Farrell, 1987; Silva & Epstein, 2010, 2012). However, these studies were limited in that they used click evoked ABRs, which are not frequency specific, or tone-burst ABRs, which are not very robust. These studies also have some limitations related to the signal processing techniques used. With these issues in mind, the present work attempts to overcome some of these shortcomings by using one octave-band chirp stimuli with center frequencies of 1000 Hz and 4000 Hz, and also by improving the signal processing

procedures used through a modified version of Silva (2009) that computes weighted averages based on Bayesian inference.

In this first chapter a brief description of the anatomy and physiology of the periphery auditory system and its relevance for loudness perception is presented. As well, an introduction to auditory evoked responses is provided, with a focus on the ABR and how it is recorded.

1.1 General Auditory Anatomy and Physiology

In this section, the general anatomy and physiology of the different parts of the ear from the external ear to the inner ear are introduced.

1.1.1 Outer ear and middle ear

The peripheral auditory system consists of three sections: the outer ear, the middle ear, and the inner ear. Figure 1-1 shows a general schematic overview of the peripheral auditory system. The first stage that significantly affects the acoustic signal properties is the outer ear, including the pinna and the auditory canal. As the sound is transmitted to the middle ear, sound pressure in the frequency range of 2 kHz to 7 kHz is amplified on the order of 15-20 dB (Pickles, 2012).

Sound transmission down the ear canal causes the tympanic membrane (the eardrum) to vibrate. The tympanic membrane and the three miniscule bones, the incus, malleus, and stapes, which together are termed the ossicles, constitute the middle ear.

There is an impedance mismatch between the air-filled space of the middle ear and fluids of the inner ear which means that more pressure is needed for signal propagation in the inner ear in comparison with the middle ear. Therefore, direct impinging of sound energy in the air on the inner ear fluid might cause energy loss. The main purpose of the middle ear is to compensate for the impedance mismatch and to efficiently convey the airborne sound to the liquid that fills the inner ear, where the neural process of hearing begins (reviewed in Pickles, 2012; Yost, 2013).

One significant way that impedance matching through the middle ear is achieved is by the tympanic membrane having a much larger area compared to that of the oval window (ratio of about 12:1 in humans). As pressure is defined as force per unit area, the same amount of force applied to the smaller area of the oval window results in larger pressure at the oval window compared to the tympanic membrane (Pickles, 2012).

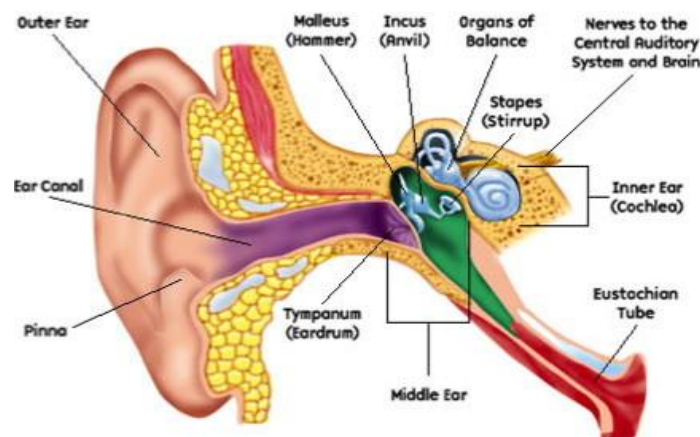


Figure 1-1: a general schematic overview of the peripheral auditory system (Schnupp, Nelken, & King, 2010).

1.1.2 Cochlea (inner ear)

The cochlea in the inner ear is divided into three fluid filled chambers, named the scala media, scala tympani, and scala vestibuli, separated by two membranes called Reissner's membrane and the basilar membrane. Inside the cochlea and above the basilar membrane lies the organ of Corti which contains the sensory receptors called the hair cells (Figure 1-2). There are two types of hair cells, inner hair cells and outer hair cells, each with specific functions. In humans, there are 3,500 inner hair cells located in one row, which convey the afferent information to the brainstem. In addition, there are 12,000 outer hair cells arranged in three rows, whose major role is to mediate the active processes in the cochlea (Hudspeth, 2014).

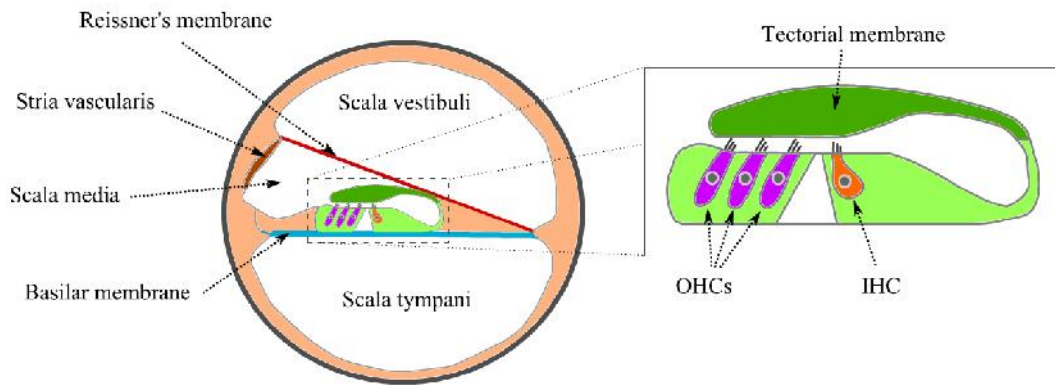


Figure 1-2: Cross-section of the cochlea (Schnupp et al., 2011).

When the cochlea is stimulated, the pressure of the fluid at the base of the scala vestibule increases and decreases as a result of back and forth movements of stapes. The resulting pressure variation along the basilar membrane evokes travelling waves or mechanical disturbance across the basilar membrane from the base of the cochlea towards the apex, rather than moving the basilar membrane as a unit (Figure1-3). The physical properties along the basilar membrane vary from basal regions to apical regions; the apex end is broad, heavy and flaccid while the base end is narrow, light and taut. As a result, excitation patterns vary along the basilar membrane as a function of stimulus frequency; the apex end is most sensitive to the low-frequency stimuli and basal regions respond best to high- frequency stimuli. Therefore, each place along the cochlea is maximally excited by a specific frequency, called its characteristic frequency. As is shown in Figure 1-3, once the traveling wave reaches the characteristic place for its frequency and resonates, wave propagation stops abruptly (Hudspeth, 2014). Upward and downward movements of the basilar membrane causes the hair cells located along the basilar membrane to move. This movement causes electrical activation of inner hair cells. Given that specific frequency input causes maximal vibration at specific locations corresponding to those

characteristic frequencies, information transmission to the brainstem contains frequency information in a place code.

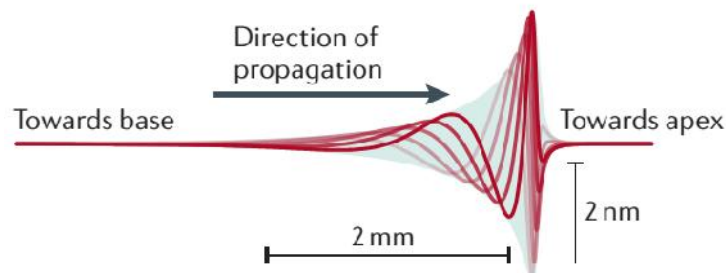


Figure 1-3: The membrane does not move as a unit; instead, successive waves propagate from the base of the cochlea towards its apex (Hudspeth, 2014).

Outer hair cells contribute to active processes in the cochlea in order to improve hearing in a number of ways (Robles & Ruggero, 2001; M a Ruggero & Rich, 1991). These active process in the cochlea lead to remarkable characteristics of audition (reviewed in Hudspeth, 2014; Hudspeth, 2008). For example, active processes in the cochlea lead to high frequency resolution, on the order of about $1/360^{\text{th}}$ of an octave. High sensitivity to weak signals and the ability to amplify quiet inputs by several hundred fold are the other remarkable features of the cochlea. This amplification is not linear as a function of sound intensity but nonlinear, as the healthy cochlea is much more sensitive to low-level sounds. This nonlinear compression characteristic of the active process of the cochlea enables the encoding of an extremely broad range of sound amplitudes to a dynamic range of about 120 dB (Hudspeth, 2014; Moukos, Balatsouras, & Nikolopoulos, 2013).

1.1.2.1 Cochlea Amplifier

It is well documented that the outer hair cells of the cochlea play a crucial role in providing nonlinear amplification of the fluid fluctuations along the basilar membrane (Musiek & Baran, 2007). Although maximum excitation along the basilar membrane occurs at the specific region of the characteristic frequency, the excitation pattern varies as a function of the intensity of the stimulus. Figure 1-4 represents the excitation pattern along the basilar membrane in a chinchilla stimulated by a 10 KHz stimulus (Ruggero & Rich, 1991). The dependency of the basilar membrane excitation peak location and pattern on level is obvious. Frequency tuning is sharper at lower stimulus levels compared to higher stimulus levels.

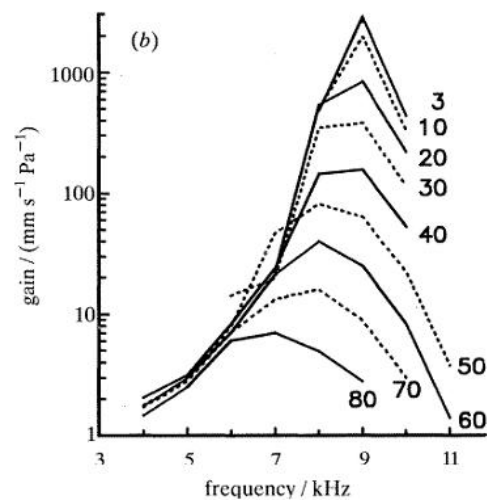


Figure 1-4: Excitation pattern of basilar membrane to a 10 KHz stimulus. It is clear that at lower levels, frequency tuning is sharper while at higher levels, it is more broadly tuned (Ruggero & Rich, 1991).

The importance of the nonlinear amplification becomes obvious when the outer hair cells are damaged. For example, Figure 1-5 shows the linearization of the excitation pattern along the basilar membrane without outer hair cell activity, which leads to a reduction in or elimination of

the dependency of frequency tuning on the stimulus level and also loss of the dynamic range (Robles & Ruggero, 2001) .

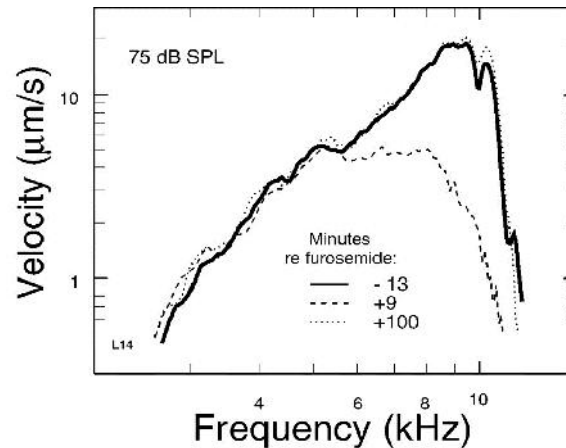


Figure 1-5: Frequency spectra of BM responses to 75-dB SPL clicks in chinchilla before (solid line) and after (dashed line) the intravenous injection of furosemide. It is obvious that after injection, frequency tuning is reduced and basilar membrane response to stimulus is linear (Robles & Ruggero, 2001).

Of particular concern is how the cochlear nonlinearity affects higher levels of auditory processing, that is, how perception changes if cochlear amplification is no longer present. For example, people who have loss of healthy outer hair cells suffer from a reduced basilar membrane dynamic range. Consequently, the dynamic range of the higher-level processing in the auditory system is also decreased when the cochlear nonlinear amplification is no longer present (Yates, Winter, & Robertson, 1990).

1.2 Loudness Growth

Loudness is a subjective experience related to sound intensity. As discussed above, there is a nonlinear relation between loudness and sound intensity, which depends considerably on the stimulus frequency. Two terms are used to describe or measure the perceived loudness of a

sound: phon and sone. The phon scale of loudness, which is the level in dB SPL that is perceived to be equal in loudness to a loudness-matched 1000 Hz tone, was devised in order to compare the loudness of different sounds with different frequencies. For this purpose, the standard tone, a 1000 Hz pure tone, was presented at different levels, expressed in dB SPL and listeners were asked to vary the level of the comparison tones presented at various other frequencies until both the standard tone and the comparison tone were perceived as equally loud. Figure 1-6 shows the relation between loudness and intensity as a function of frequency. For instance, a 1000 Hz tone at 10 dB SPL intensity is judged to be equal in loudness to a 63 Hz tone at 40 dB SPL intensity. To investigate the effect of changing intensity in dB at one specific frequency on the perception of loudness, a sone was defined as the loudness of a 1000 Hz tone presented at 40 dB SPL or, in other words, 1 sone is equal to a 40 phon loudness (Hamill & Price, 2008). Therefore, a stimulus with loudness of n sones is perceived as n times as loud as 1 sone, that is, n times as loud as the 1000 Hz, 40 dB SPL.

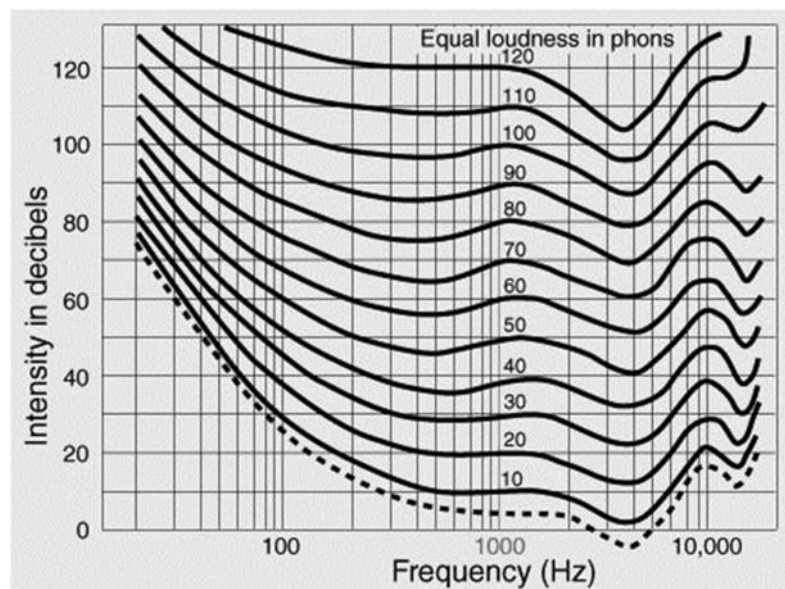


Figure 1-6: Equal loudness contours (Hamill & Price, 2008).

1.2.1 Loudness Growth Models for Normal Listeners

There are some mathematical models describing the relation between loudness growth and stimulus intensity. One of the first models was introduced by S. Stevens (Stevens, 1955, 1957), who modeled loudness growth as a power function of the sound pressure of the stimuli:

$$L = 0.01 P^{0.6} \quad (1-1)$$

where P is the sound pressure in micropascals and L is the estimation of the loudness in sons. The main inaccuracy of this model is in the estimation of loudness at low stimulus levels, close to the hearing threshold. Hellman & Zwislock (1961) tried to modify this shortcoming by using a constant value, P₀ which is an estimation of the effective threshold:

$$L = 0.01 (P - P_0)^{0.6} \quad (1 - 2)$$

Although these two models are different at low stimulus levels, they essentially converge at higher levels (Figure 1-7).

However, more investigations about the loudness growth over time showed that the exponent factor of loudness growth is different at different stimulus levels in people with normal hearing; it is larger than 2 close to the threshold, lower than 0.6 at moderate stimulus levels, and even lower at high stimulus levels. So, more attempts were made to develop a loudness growth model that was based on these new findings. More recently, the INflected EXponential (INEX) loudness model has been proposed based on observations of many studies (e.g. Robinson, 1957; Hellman & Zwislocki, 1961; Stevens, 1972; Buus, Florentine, & Poulsen, 1997; Buus & Florentine, 2001). It attempts to account for the varying slope of the loudness growth function at low, moderate and high levels (Buus & Florentine, 2001; Florentine & Epstein, 2006):

$$f(L) = 1.7058 * 10^{-9} * L^5 - 6.587 * 10^{-7} * L^4 + 9.7515 * 10^{-5} * L^3 - 6.6964 * 10^{-3} * L^2 + 0.2367 * L - 3.4831 \quad (1 - 3)$$

where $f(L)$ is the loudness in sones and L is the level in dB SPL. Figure 1-7 demonstrates the loudness growth functions of these models for people with normal hearing.

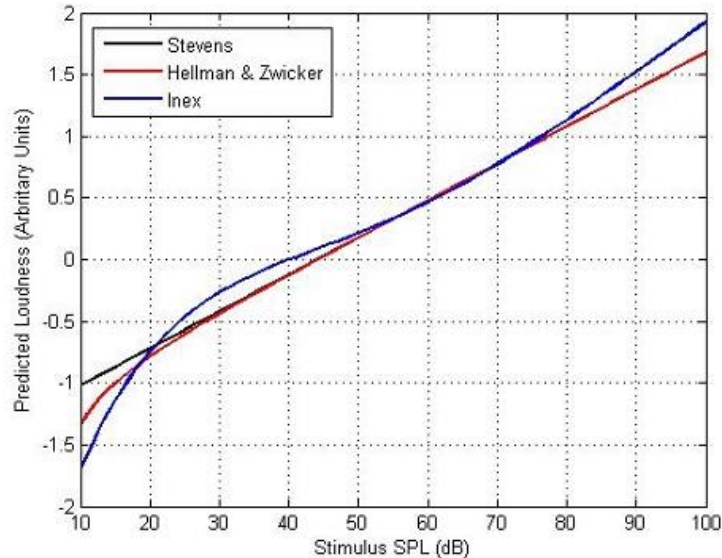


Figure 1-7: Comparing three loudness growth functions.

1.2.2 Psychoacoustical Procedures for Estimating Loudness Growth

Over the years, many researchers have developed procedures to measure loudness for the purpose of hearing aid fitting (Elberling, 1999). Two major psychoacoustical procedures are currently used to estimate loudness growth in humans: Cross-Modality Matching (CMM) and Absolute Magnitude Estimation (AME). In the CMM procedure, the participants are asked to match the loudness of sounds with another perceptual cue (e.g., to mark on a string the point that represents the loudness of the sound from very quiet to very loud), while in the AME procedure a numerical value is assigned to the perceived loudness.

However, there is considerable variability among the published results for loudness scaling obtained with the different procedures in both normal hearing and hearing impaired listeners (Elberling 1999). Bias is one limitation in these procedures. Moreover, it is essential for the participants to be conscious and to be able to comprehend the task, which is not always easy for

children, the elderly, and those with cognitive impairment. In addition, even normal people may have inconsistent perceptual judgments due to many factors such as stress or exhaustion (Silva & Epstein, 2010).

On the other hand, current clinical approaches to estimate the loudness growth function through psychoacoustical methods are limited to obtaining three data points: threshold, most comfortable loudness, and uncomfortable loudness (for review, see Smeds & Leijon, 2011). However, it is well documented that loudness growth functions can be very different among individuals with similar audiometry measurements (Elberling, 1999).

Therefore, it has been suggested that applying objective procedures could overcome these shortcomings. In particular, electrophysiological methods such as estimation of loudness growth functions with auditory brainstem responses or otoacoustic emissions have been explored in a number of research projects (e.g. Davidson, Wall, & Goodman, 1990; Silva & Epstein, 2010, 2012).

1.3 Auditory Brainstem Response

The measured electrical response of the auditory system generated in response to an acoustic stimulus to the ear is called the auditory evoked potential (AEP). The AEP shows a series of distinct peaks arising from successive places along the auditory pathway. Figure 1-8 shows the AEP waveform. The AEP waveform consists of three different parts, called auditory brainstem response (ABR), middle latency response (MLR) and the late latency response (LLR) (Melcher, 2009).

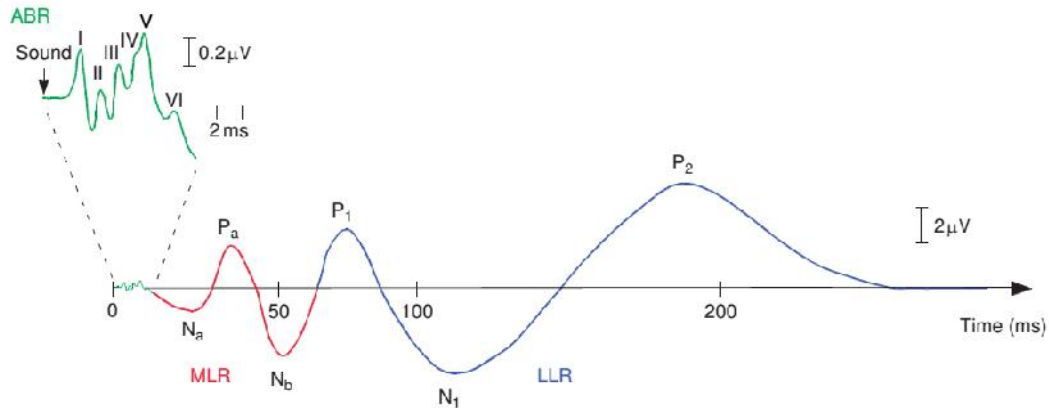


Figure 1-8: A schematic of the auditory evoked potential signal in human. The ABR response is up to approximately 20 ms, the MLR is between 20 and 40 ms, and the LLR is between 50 to 100 ms after stimulus onset (Melcher, 2009).

The ABR originates from the periphery and brainstem nuclei (Arnold, 2000). First recorded by Jewett (1971), the ABR has been widely used to assess neural disorders in the auditory pathways. The ABR also provides an objective method for evaluating hearing sensitivity for newborns and young children, and also for the elderly and people with cognitive impairment. The ABR response is clinically useful because it is similar across individuals and is little affected by level of conscious awareness (Arnold, 2000).

The peaks of the ABR are labeled in a sequence by Roman numerals as wave I to wave VII (Figure 1-9). It is generally agreed that waves I and II are both generated in the auditory nerve, wave III originates from the cochlear nucleus and wave IV from the superior olivary complex (SOC). Wave V is assumed to originate from the lateral lemniscus (LL) as it terminates in the inferior colliculus (IC) (Arnold, 2000). Wave V is used most often in clinical applications and research as it is the biggest and the most reliable peak of the ABR response. Both latency and peak amplitude of these waves are used to investigate whether a person's ABR is normal. It should also be noted that the ABR morphology changes in a predictable manner when the

stimulus intensity increases, specifically, peak amplitudes increase with increasing stimulus intensity (Melcher, 2009).

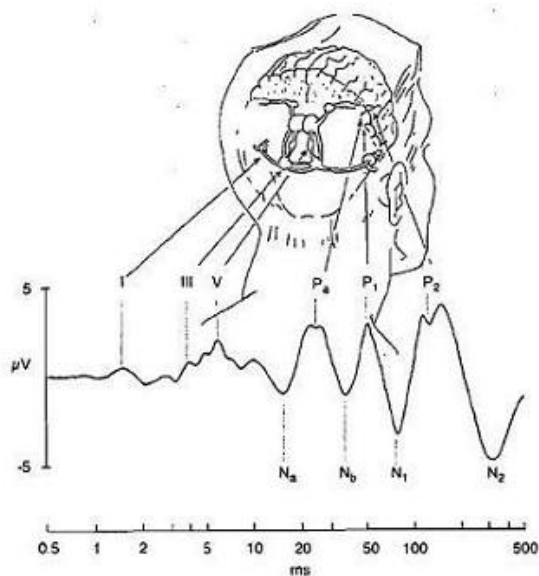


Figure 1-9: Recorded ABR waveform (Burkard, Eggermont, & Don, 2007).

1.3.1 ABR Stimuli

The ABR is affected by various characteristics of the stimulus such as frequency and intensity. For example, stiffness differences along the cochlea cause maximum excitation of the basilar membrane to occur several milliseconds later for lower frequency stimuli, which are encoded at the apical end of the cochlea, compared to high frequency stimuli, which cause maximum displacement at the basal end of the cochlea (Hudspeth, 2014; von Békésy, 1990; Figure 1-10). This phenomenon is called temporal dispersion. In addition to stimulus frequency, stimulus intensity has an obvious effect on the morphological features of ABR such as the latency and the amplitude of wave V (Neely, Norton, Gorga, & Jesteadt, 1988; Ruggero & Temchin, 2007).

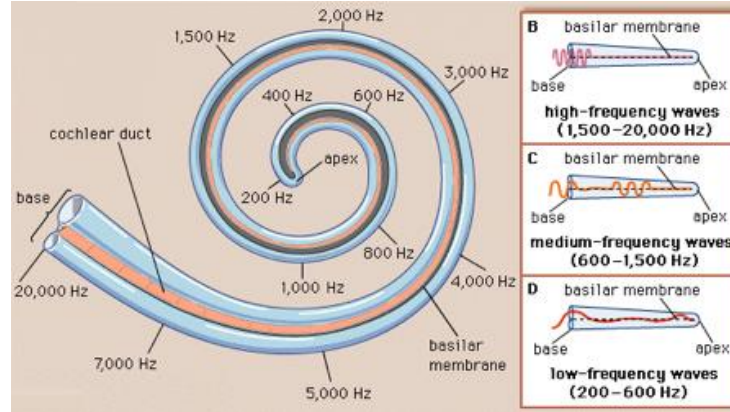


Figure 1-10: The tonotopic map along the basilar membrane.

Click stimuli are the most common type of stimuli used to elicit the ABR response for both neurodiagnostic and audiological purposes (e.g. Musiek, Borenstein, Hall, & Schwabe, 1994). Click stimuli are broad-band spectrum signals and therefore, in theory, the whole basilar membrane is stimulated by click stimuli, which makes them unsuitable for getting information about the specific audiometric frequencies. Figure 1-11 shows the time-frequency representation of the click ABR for the first 4 ms (Kiang, 1975). It is obvious that, due to temporal dispersion, as time progresses, basilar membrane displacements relative to lower frequencies occur with wider peaks and smaller amplitude responses compared to the sharp peak responses of the first excitations in higher frequency regions. Sharper peaks in basal regions elicit more synchronous responses compared to the broader peaks of the apical regions (Fobel & Dau, 2004). Furthermore, generated activity in more synchronous basal regions will be out of phase with activity in the apical regions (Coats & Martin, 1977; Neely et al., 1988). Therefore, the less synchronous responses of apical regions and phase cancellation between apical and basal regions result in the ABR signal reflecting mostly activity from the basal regions (Eggermont & Don,

1980; Neely et al., 1988). So the ABR response to a click stimulus which consists of different frequency components is not entirely synchronous (Fobel & Dau, 2004).

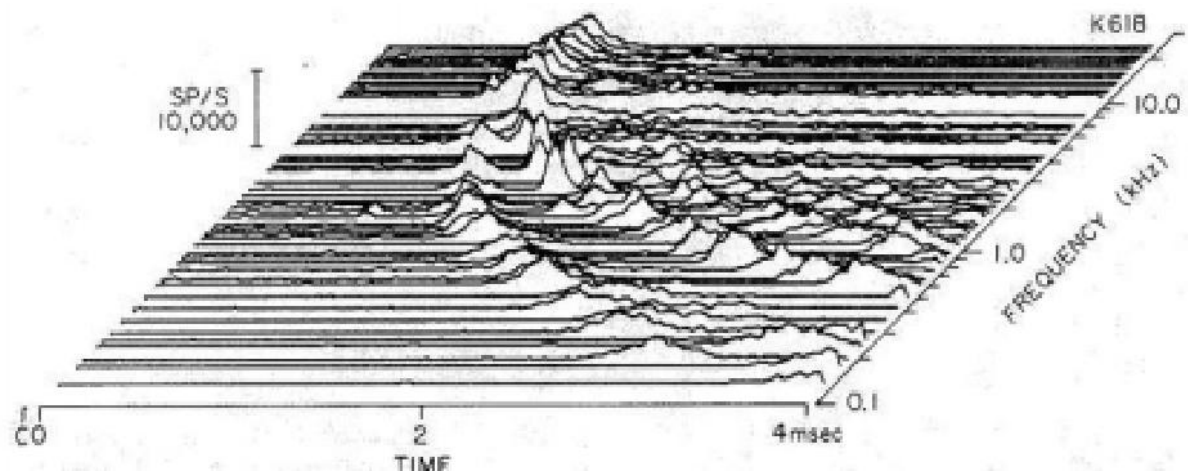


Figure 1-11: Time-Frequency representation on the basilar membrane of the click ABR for the first 4 ms. It is obvious that each frequency component of the click stimuli is separated in time as the result of temporal dispersion (Kiang, 1975).

The second typically-used stimulus is the tone burst, which is a frequency-specific transient stimulus and ideally excites the specific tonotopic region on the basilar membrane relative to the stimulus frequency (Hall, 2006). However, it is well documented that abrupt stimulus onsets create spectral splatter such that short tone bursts contain other unwanted frequencies above and below the tone's characteristic frequency, which also generate responses (Hall, 2006). Decreased frequency specificity of the ABR has been reported for people with normal hearing for tone-burst intensities of 40-50 dB nHL or higher and for frequencies of 500, 1000, 2000 and 4000 Hz compared to ABR to the other stimuli like the tone burst stimuli with notched noise masking (Orsini, 2004; Stapells, Linden, Suffield, Hamel, & Picton, 1984).

Furthermore, tone burst stimuli tend to excites smaller numbers of neurons than broad band signals, which results in relatively low synchronized neural responses. Therefore, tone burst ABRs have a significantly lower signal to noise ratio compared to click ABRs (Burkard, Eggermont, & Don, 2007; Hall, 2006). Reduced frequency specificity and low reliability of the ABR response to tone burst stimuli has led to debates among researchers as to whether tone-burst stimuli are sufficient to elicit the ABR (Stapells, Galambos, Costello, & Makeig, 1988; Stapells et al., 1984).

So, neither the tone burst nor the click stimulus provides the ideal neural synchrony needed for a robust ABR measurement (Fobel & Dau, 2004). Thus another class of stimuli has been developed, the chirp stimulus, which creates more synchronous neural activity and consequently a more reliable ABR (Dau, Wegner, Mellert, & Kollmeier, 2000; Elberling, Don, Cebulla, & Stürzebecher, 2007; Fobel & Dau, 2004; Wegner & Dau, 2002).

1.3.1.1 Chirp Stimuli

As discussed above, the tonotopic nature of the cochlea leads to temporal delay in excitation of the apical regions compared to the basal regions. There are two main approaches to align the activity along the cochlea in order to improve the temporal synchronization of the neural units that contribute to the total ABR, output compensation and input compensation (Elberling et al., 2007). Don and colleagues (Don, Ponton, Eggermont, & Masuda, 1994) developed the output compensation technique in which the ABR is measured in narrow frequency bands, each band time shifted by the appropriate amount, and the time-shifted signals are then added together. The obtained signal is called the Stacked ABR (Figure1-12). Although the Stacked ABR shows a more synchronous response that is significantly larger in amplitude compared to the common

click ABR, it has not been clinically popular due to the necessity of a specialized recording procedure (Elberling et al., 2007).

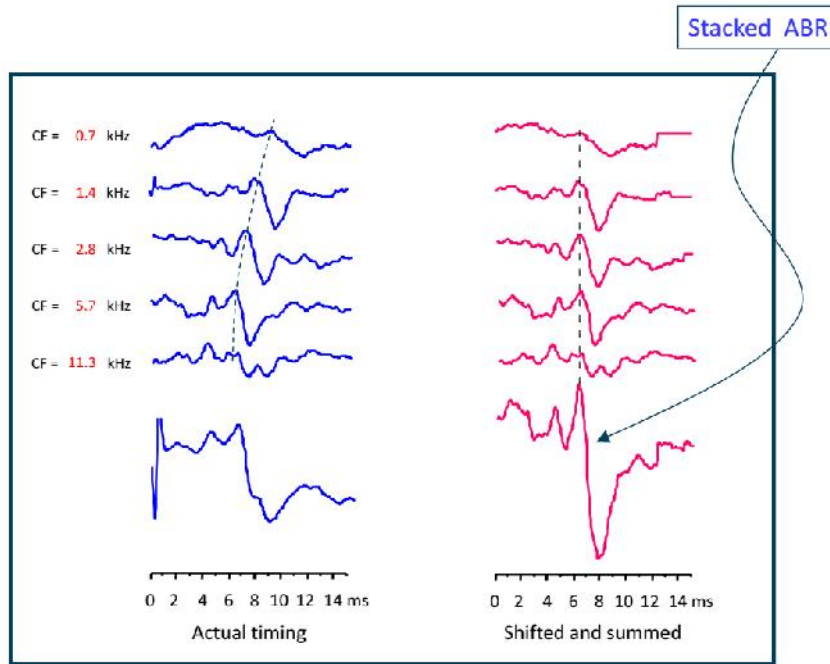


Figure 1-12: Narrow frequency bands ABRs (left) are shifted summed to construct the Stacked ABR (right) (Don, 2002).

On the other hand, the input compensation approach is based on stimulus rather than response synchronization. In this method, the different frequency components of the stimulus are time shifted in reverse according to their time shift on the basilar membrane; higher frequencies are sent into the cochlea a bit later than the lower frequencies (Elberling et al., 2007). As a result, different neural units along the cochlea are excited simultaneously and no or little temporal dispersion will occur. Figure 1-13 shows a comparison between click and chirp stimuli.

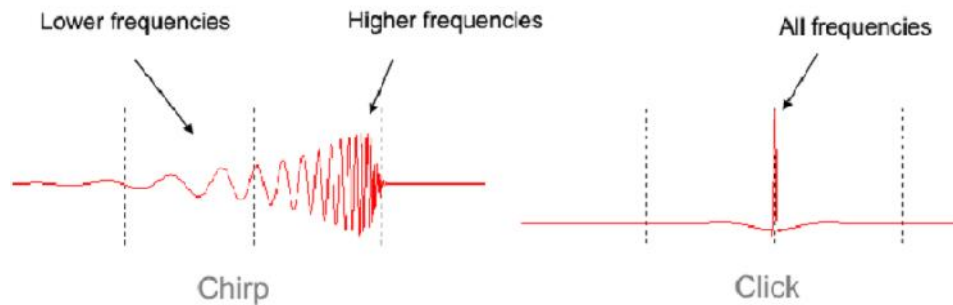


Figure 1-13: Chirp (left) and click (right) stimulus (Jill, 2010).

There are several models of the human cochlea delay that have been used for constructing chirp stimuli. Some examples are: the cochlear model of de Boer (1991) which was obtained by using the Greenwood (1990) cochlear tonotopic map; the model based on tone-burst ABR recordings (Gorga, Kaminski, Beauchaine, & Jesteadt, 1988; Neely et al., 1988); and the model based on derived-band ABR recordings (Don, Kwong, & Tanaka, 2005). Generally, a cochlear delay model can be defined as a power law function according to:

$$\tau = k \cdot f^{-d} \quad (1 - 4)$$

where τ is the delay in seconds, f is the frequency in Hz and k and d are constant values that can be determined by different data, such as tone-burst ABRs, otoacoustic emission, etc. (Elberling, Callø, & Don, 2010). Figure 1-14 represents four different cochlea delay models.

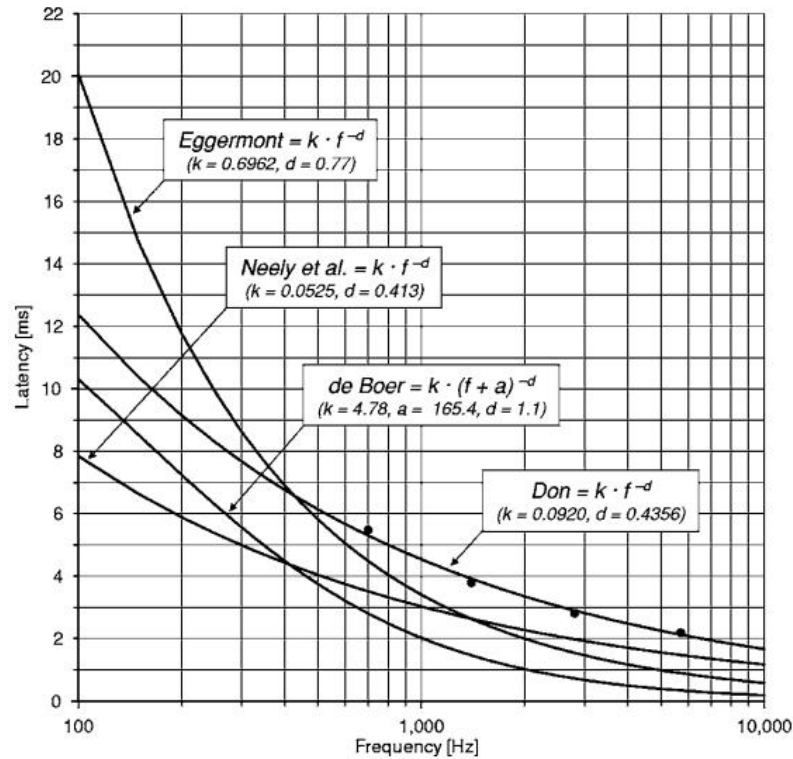


Figure 1-14: Four different cochlea delay models extracted from narrow-band

ACAP of (Eggermont, 1979), tone-burst ABR of (Neely et al., 1988),

narrow-band ABR of (Don, Kwong, & Tanaka, 2005) and a cochlear model of (de Boer, 1980). Reprinted from Elberling et al. (2007).

Many researchers attempted to find the most efficient chirp stimulus based on different delay models in order to evoke the most robust ABR in humans. One of the first attempts to design chirp stimuli was done by Lütkenhöner et al. (1990), which was based on the estimation of cochlea traveling time using the tone-burst ABRs (Elberling et al., 2007). Elberling et al. (2007) and Fobel & Dau (2004) also have applied frequency-specific ABRs to design the chirp stimuli. Another chirp stimulus was developed by Dau et al. (2000) using the linear cochlea model of de Boer (1980). More recently, other researchers (e.g. Elberling et al., 2007; Fobel & Dau, 2004; Stürzebecher, Cebulla, Elberling, & Berger, 2006) also used linear models of cochlea

function in order to design chirp stimuli. Furthermore, Fobel & Dau (2004) applied a cochlea delay model derived from stimulus-frequency otoacoustic emission latency data from Shera & Guinan (2000), and Elberling and colleagues (Elberling et al., 2007; Elberling & Don, 2008) used derived-band ABR latencies to construct chirp stimuli.

The efficiency of using chirp stimuli to evoke ABR compared to other stimuli in terms of eliciting a larger wave-V amplitude is well documented (e.g. Dau et al., 2000; Elberling et al., 2010, 2007; Elberling & Don, 2007, 2008, 2010; Ferm, Lightfoot, & Stevens, 2013; Fobel & Dau, 2004; Gøtsche-Rasmussen, Poulsen, & Elberling, 2012; Maloff & Hood, 2014; Ribeiro, Rodrigues, & Lewis, 2012; Rodrigues, Ramos, & Lewis, 2013; Stuart & Cobb, 2014).

Furthermore, some studies have used chirp stimuli to estimate hearing thresholds in infants and children (e.g. Ferm, Lightfoot, & Stevens, 2013; Mühler, Rahne, & Verhey, 2013; Soares, Nakazawa, Ishikawa, Sato, & Honda, 2014; Xu, Cheng, & Yao, 2014; Zirn et al., 2014). However, no studies have been done to investigate the feasibility of using chirp stimuli in combination with ABR recordings to objectively estimate loudness growth. This is the main goal of this study.

Chirp stimuli are now applied in clinics to evoke the ABR. In 2007, the CE-chirp, named in honor of Claus Elberling, was implemented into the diagnostic EP platform used in clinics. This has considerably reduced test time and made interpretation of the results easier for clinicians. For example, wave V amplitudes up to twice as large as those measured using traditional clicks or tone bursts can be achieved with both the broadband CE-Chirp and frequency-specific narrow-band CE-Chirp (Elberling & Don, 2008).

1.3.2 ABR Signal Processing

Although there are many applications of the auditory brainstem response, its low signal to noise ratio has remained the major drawback of using this evoked potential signal. Thus, many attempts have been made to recognize the noise sources and develop the analysis methods to increase the signal to noise ratio. The recorded ABR signal is generally modeled (equation 1-5) as the superposition of two independent components: the evoked potential response of the acoustic stimulation $s_A(t)$, which is defined as a deterministic component, and a non-stationary stochastic zero-mean Gaussian noise $\eta(t, k)$, whose properties can vary with trial number, k (Elberling & Wahlgreen, 1985).

$$x_A(t, k) = s_A(t) + \eta(t, k) \quad (1 - 5)$$

The main sources of the physiological background noise are electrical activities of both neural and muscular origin. Although subjects are asked to minimize their movements to control the background noise originating from the subject, large background noise relative to the evoked potential is still typically observed (Elberling & Wahlgreen, 1985). The classical technique of averaging many trials of the EEG response to the same stimulus in the time domain is the most commonly applied method for improving the signal to noise ratio (Don & Elberling, 1994). However, it is well documented that this classical averaging technique is not successful enough to retrieve an ABR evoked potential signal from a non-stationary background noise. Unfortunately, the assumption that the background noise of the recorded ABR signal is stationary with constant properties over time is false (Elberling & Wahlgreen, 1985; Elberling & Don, 1983). There are many other noise sources in environment commonly hard to identify. Electromagnetic noise from nearby equipment and power line noise are the simple examples of none physiological sources of noise (Marcoux & Kurtz, 2012).

Elberling & Wahlgreen (1985) developed the weighted averaging method by using Bayesian methods to estimate the deterministic component of the recorded ABR signal from the Gaussian background noise. Based on the principle of Bayesian inference, adding new information to prior knowledge through the likelihood function will produce updated posterior information, which is applicable for the averaging method where new data are continuously added to the existing data. Therefore, assuming that the background noise has a Gaussian distribution, each individual sweep used in the averaging procedure is weighted proportionally to its precision based on Bayesian inference (equation 2-9). In this regard, the precision of each sweep is defined by the inverse of the variance of the recorded sweep (Elberling & Wahlgreen, 1985). These consecutive procedures are well explained by the following formulas (Equations: 1-6, 1-7, 1-8). In the following equations, x_i indicates the recorded signal, V_i is the variance of the background noise and \widehat{E}_i denotes the Bayesian estimation of the evoked potential after introducing the i th trial. So, the estimated potential after the first trial is

$$\widehat{E}_1 = \left(\frac{x_1}{V_1} \right) \cdot \frac{1}{C_1}; \quad C_1 = \frac{1}{V_1} \quad (1 - 6)$$

And after the second trial is

$$\widehat{E}_2 = \left(\frac{x_1}{V_1} + \frac{x_2}{V_2} \right) \cdot \frac{1}{C_2}; \quad C_2 = \frac{1}{V_1} + \frac{1}{V_2} \quad (1 - 7)$$

Similarly, after the n th block, \widehat{EP}_n is:

$$\widehat{E}_n = \left(\frac{x_1}{V_1} + \frac{x_2}{V_2} + \dots + \frac{x_n}{V_n} \right) \cdot \frac{1}{C_n}; \quad C_n = \frac{1}{V_1} + \frac{1}{V_2} + \dots + \frac{1}{V_n} \quad (1 - 8)$$

Equation 1-8 defines how \widehat{EP} is estimated based on the Bayesian inference, which can be written as equation 1-9 and compared with the normal averaging with equation 1-10:

$$\widehat{E}_n = \frac{1}{n} \cdot \left(\frac{x_1}{V_1} + \frac{x_2}{V_2} + \dots + \frac{x_n}{V_n} \right) \cdot \frac{n}{C_n} \quad (1 - 9)$$

$$\widehat{E}_n = \frac{1}{n} \cdot \left(\frac{x_1}{V_1} + \frac{x_2}{V_2} + \dots + \frac{x_n}{V_n} \right) \quad (1 - 10)$$

It is obvious that if the background noise is stationary with constant variance, both weighted averaging and normal averaging achieve identical results. The advantage of weighted averaging compared to traditional averaging is well documented; for example, as is shown in Figure 1-15, if there is a sudden increase in the amount of noise, the weighted averaging method based on Bayesian inference will reduce the effects of the sudden noise to close to the theoretical value, even though both methods produce similar results in the absence of sudden increases in the amount of noise (shown up to 2000 sweeps in Figure 1-15) (Don & Elberling, 1994).

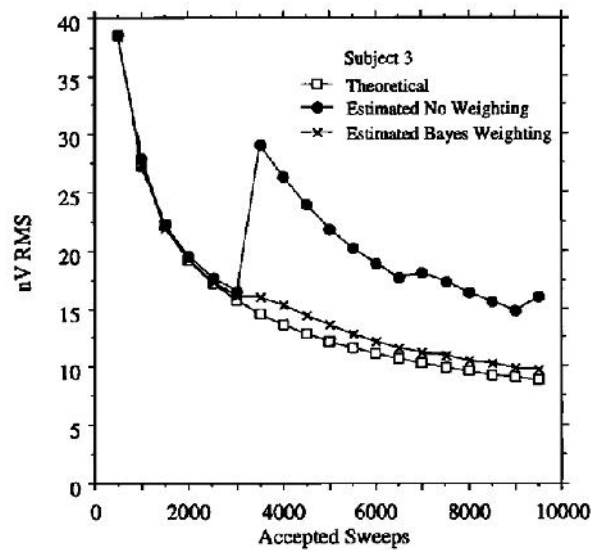


Figure 1-15: Comparison between different methods of averaging on a data with a sudden increasing amount of noise (Don & Elberling, 1994).

However, it is impossible to measure the variance of the background noise in a single sweep confidently. Elberling and Don (1983) introduced the fixed single point method to estimate the variance of the background noise in blocks of sweeps instead of one sweep,

assuming that each block is locally stationary. In this method, for each trial within each block, an arbitrary fixed post-stimulus time point, t_0 , is selected and the variance of the corresponding block, $\sigma_{\eta}^2(k)$, is defined by calculating the variance across the selected points of the trials in that block (equation 1-11).

$$\sigma_{\eta}^2(k) = \frac{1}{k_1 - k_0 - 1} \sum_{m=k_0}^{k_1} (x_{A}(t_0, m) - \overline{x_{A}(t_0)})^2 \quad \text{for } k_0 \leq k \leq k_1 \quad (1 - 11)$$

where $\overline{x_{A}(t_0)}$ is the normal sample mean of the recorded ABR voltage at the selected reference point of t_0 .

Nevertheless, since in this method of measuring variance, the entire block is weighted as a unit, the computed weighting factor may be not adequate enough if the variation was large among the sweeps of that block. For this reason, a modification was done by Don & Elberling (1994) to reduce the number of sweeps in each block but use multiple fixed points (L fixed pointes) equally spaced by Δ samples apart, instead of a single point within each sweep. This method assumes a discrete number of noise sources with different power instead of single noise source. Therefore, the multiple fixed point method has the advantage of better controlling noise variations by weighting smaller blocks of sweeps (equation 1-12).

$$\sigma_{\eta}^2(k) = \frac{1}{L} \sum_{n=0}^{L-1} \frac{1}{k_1 - k_0 - 1} \sum_{m=k_0}^{k_1} (x(t \cdot \Delta, m) - \overline{x(t \cdot \Delta)})^2 \quad \text{for } k_0 \leq k \leq k_1 \quad (1 - 12)$$

Based on the equation 1-12, L estimates of the noise variance within each block of trials are calculated by the inner summation. Then the L noise variances of each block are averaged through the outer summation to yield the sample mean within that block.

Furthermore, Silva (2009) has recently modified previous methods by segmenting the data into a variable number of trials. It can then be tested whether local stationarity is maintained

when the number of trials is increased. For this purpose, a series of F-tests are used recursively to estimate the total number of independent noise sources. By assuming a minimum number of trials, M_m , for which the noise source remains stationary, the current noise source variance can be estimated by equation (1-12). The F-test of the relation between the current and the previous noise variances is then calculated to find out the likelihood that the current noise source power lies within a given confidence interval of the previous one:

$$F(D_{\eta(i-1)}, D_{\eta}) = \frac{\hat{\sigma}_{\eta(i-1)}^2}{\hat{\sigma}_{\eta}^2} \quad (1 - 13)$$

$$D_{\eta i} = LM_m - 1 ; D_{\eta(i-1)} = LM_{\eta(i-1)} - 1 \quad (1 - 14)$$

where L is the number of fixed samples applied in equation 1-12 to estimate the noise source variance. If the test statistic is not within the confidence interval of the previous noise source power, it can be concluded that there is an independent new noise source. Otherwise, the current estimate is updated applying recursive averaging:

$$\hat{\sigma}_{\eta i}^{2'} = \frac{Q\hat{\sigma}_{\eta(i-1)}^2 + \hat{\sigma}_{\eta i}^2}{Q + 1} ; M'_{\eta i} = M_{\eta i} + M_{\eta(i-1)} \quad (1 - 15)$$

$$Q = \frac{\bar{M}_{\eta(i-1)}}{M_m} \quad (1 - 16)$$

where $\bar{M}_{\eta(i-1)}$ is the total number of estimated variances used to estimate the variance of the previous block. Segmentation of the data in this manner defines dynamic areas of stationarity for noise sources (Silva, 2009).

1.4. Previous studies of using ABR to evaluate loudness growth

Over the years, many studies attempted to find a correlation between different features of the ABR as an objective approach of assessing loudness growth functions and psychoacoustical procedures of loudness growth measurement, specifically in order to use in hearing aid fitting.

For this purpose, the most common landmark of ABR measured as a function of stimulus intensity is the wave V latency and amplitude.

One of the first attempts was done by Pratt & Sohmer (1977), in which both ABR recording and psychoacoustic procedures were done to estimate the loudness growth in normal hearing people. The ABR stimulus was a broadband click presented at different levels from 0 to 75 dB SPL and 300 trials were recorded per level. The psychoacoustic task was done using an AME Procedure with the same stimulus. Three features, latency, amplitude and area, of each of five waves of recorded ABRs were fitted by a power function and then coefficients of the power function of each feature were averaged across the subjects to investigate the correlation between each feature and the estimated loudness growth achieved by the psychacoustical procedure. They found a correlation between psychoacoustical estimates and the calculated coefficient of the ABR amplitudes; probabilities of similarity between electrophysiological power exponents (wave I, II, III, IV & V, VI) and subjective power exponent were 99% (wave I), 80% (wave II), 50% (wave III), 10% (wave IV and V), and 20% (wave VI). However, the authors claimed that the results are inconclusive because “..a closer analysis proved this similarity superficial, since AMEs showed an appreciable inter-subject and intersession variability while the auditory nerve and brainstem responses were approximately constant.” Afterwards, Wilson and Stelmack (1982) tried to replicate the Pratt & Sohmer (1977) study but with increasing the number of recorded trials to 4000 trials for each level. They could not find any correlation between power fit coefficients of the intensity-amplitude and intensity-latency of ABR components and psychoacoustic ratings.

Davidson, Wall, & Goodman (1990) used click evoked ABRs to investigate the correlation between wave V and estimated loudness growth through AME psychoacoustic

procedures on both normal hearing and hearing impaired people. In both tasks, click stimuli with different presentation levels from 10 dB SPL to 100 dB SPL were used. The click ABRs were recorded across four sessions for each participant and averaged (about 8000 trials per level). The negative amplitude of wave V was calculated as the physiological estimation of loudness. Then, the Spearman's rank correlation coefficient was calculated between the physiological and psychoacoustical variables to test if a relationship existed. A significant correlation (NHLs ($r = 0.5 - 0.99$) and HILs ($r = 0.7 - 0.99$)) was found when all trials were averaged across all four sessions, while it was not significant within the single sessions.

In Gallego et al. (1996), electrically evoked ABRs to different levels of pulse trains were recorded (2000 trials per level) from three cochlea implant participants. Some features of the ABR morphology, such as amplitude and latency of wave III and V as a function of the intensity of the stimuli were measured. It was concluded that the amplitude of wave III and V increased as intensity of stimuli increased while no significant effect was seen on the latency of III and V. In a similar study by Gallégo et al. (1999) with cochlear implants, in addition to electrically evoked ABRs, loudness growth functions were measured behaviourally through categorical scaling. Based on their ANOVA results, there was a significant correlation between EABR wave V thresholds and perceptual thresholds. Also, their ANOVA results on wave latencies and amplitudes as a function of the presentation level of stimuli showed that there is a significant effect on waves II and V amplitudes and on wave II latency. Serpanos, O'Malley, & Gravel (1997) assessed the relation of the wave V latency of click evoked ABRs as a function of stimulus intensity and the psychoacoustical loudness measurements on both normal hearing and impaired hearing people. They revealed a correlation between wave V latency and loudness in

normal hearing people and people with a flat hearing loss but no correlation was found for hearing impaired people with a sloping hearing loss.

Some other studies tried to find the loudness discomfort level objectively, which is vital in fitting the maximum hearing-aid output level. For example, in a study by Thornton, Yardley, & Farrell (1987), auditory brainstem responses to two tone bursts of 2 kHz and 4 kHz and also to click stimuli with different levels were recorded in normal hearing subjects with the specific aim of finding a suitable objective method for determining the loudness discomfort level. They tried to find a relationship between the latency of wave V and subjective results of loudness in estimation of loudness discomfort level. However, they could not find any correlation between the wave V latency/intensity function and the loudness discomfort level. In another study, Nolan & Parker (2000) used auditory brainstem responses to a 400 Hz continuous tone stimulus in normal hearing people in order to predict loudness discomfort. Some features such as response amplitude, phase, magnitude-squared coherence and phase coherence were measured relative to the intensity of the stimuli. The only significant response for prediction of loudness discomfort level was the gradient of the amplitude intensity-function of each participant.

Although most studies used click evoked ABRs, Silva & Epstein (2010, 2012) used tone burst ABRs to assess the loudness growth objectively. Two tone-burst stimuli, 1 kHz and 4 kHz tone-burst, with different levels from 5 dB below the listener's threshold to 100 dB peSPL in steps of 5 dB were presented in at least three sessions yielding a total of at least 12000 trials per level for each frequency. In addition, two different psychoacoustic procedures of AME and CMM have been used as the reference measurements of the loudness growth. Different physiological features were calculated and the mean square error between estimated loudness growth through physiological features and standard psychoacoustical procedures were

determined. Their results revealed that loudness growth estimation obtained through some of the physiological features of recorded ABRs were close to those of standard psychoacoustical procedures with low mean square-error (MSE), which was less than 0.2 for normal hearing people. Of particular interest here is using MSE instead of using, for example, Pearson correlation as a better measure of fitness for loudness since linear correlation analysis will only evaluate the degree of correlation between the linear components of the ABR features and linear components of the loudness growth function (Epstein & Silva, 2009).

2. Methodology and experiments

In this chapter, the details of the experiments designed to estimate the loudness growth function both through a psychoacoustical procedure and through auditory brainstem response recording are described. The analyses used to estimate loudness growth for each procedure are explained as well as the analyses used to compare the estimated loudness growth from the two procedures.

2.1 Subjects

Eleven normal-hearing young adults (10 female and one male) ranging from 22 to 30 years of age (mean = 27; SD = 3.43) participated in this study. Subjects were recruited from the undergraduate psychology student database. The study was approved by the McMaster University Research Ethics Board.

2.2 General Procedure

First, the experimenter explained all the test procedures to the participant and answered any questions the participant had regarding the purpose of the study. A standard consent form was read and signed by the participant. Next, participants completed the pure tone audiometry to confirm that their hearing was normal. All participants had pure-tone thresholds within 10 dB HL for frequencies from 125 Hz to 8000 Hz. All experiments were made on the right ear of each participant.

2.3 Stimuli and Calibration

In order to measure frequency-specific auditory brainstem responses, octave band chirp stimuli were used in this study, made through octave-band filtering of a broad band CE-chirp. As it is shown in Figure 2-1, the broadband CE-chirp has a flat amplitude spectrum within five octave-bands ranging from 350 to 11300 Hz, which can be filtered by one octave-band filters (based on IEC 61260, 1995) with four different center frequencies of 500, 1000, 2000 and 4000

Hz (Gøtsche-Rasmussen et al., 2012). In the present study, two octave-band chirp stimuli with center frequencies of 1000 Hz and 4000 Hz were used. The duration of each waveform was 10 ms with normalized amplitude, and each was presented at different intensity levels between 20 dB nHL and 80 dB nHL with 10 dB steps. The stimuli are shown in Figure 2-2 and Figure 2-3. It is worth mentioning that dB HL is obtained from pure-tone audiometric thresholds referred to hearing thresholds of normal hearing young individuals while, dB nHL indicates a person's hearing relative to accepted standards for normal hearing which can be used for all kind of the stimuli.

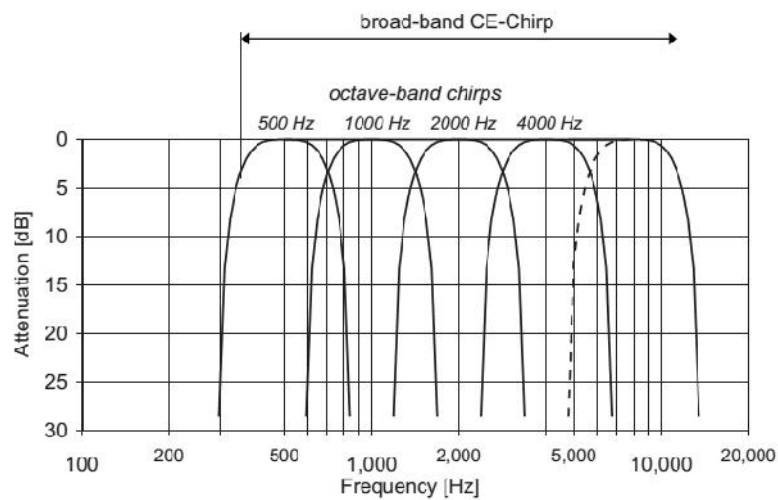


Figure 2-1: Amplitude-frequency characteristics of the filters applied for constructing CE-chirp stimuli and the four octave band chirps with four center frequencies of 500, 1000, 2000 and 4000 Hz (Elberling & Don, 2010) Only those with center frequencies of 1000 and 4000 Hz were used in the present study.

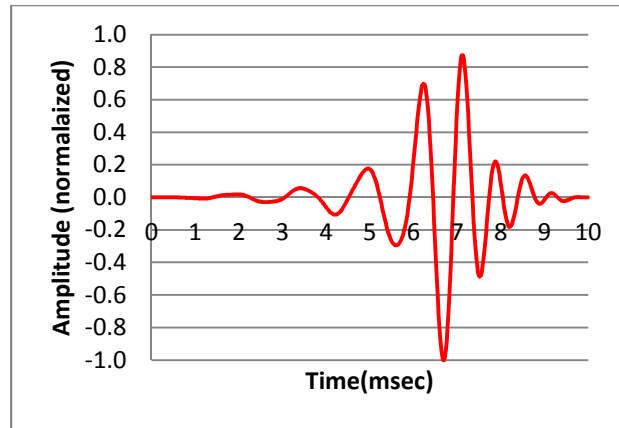


Figure 2-2: One octave-band chirp stimulus with center frequency of 1000 Hz.

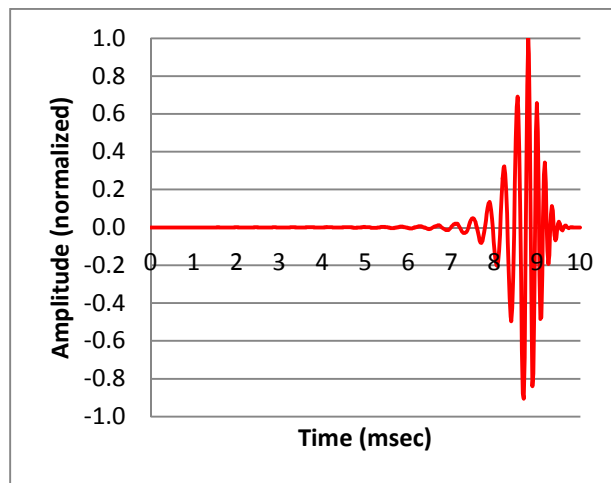


Figure 2-3: One octave-band chirp stimulus with center frequency of 4000 Hz.

Reference hearing thresholds for short-term stimuli, defined by peak-to-peak equivalent Reference Equivalent Threshold Sound Pressure Levels (peRETSPLs) according to ISO 389-6, were applied in the calibration procedure in order to ensure consistency among different results achieved with different equipment (Fedtke & Hensel, 2010; Fedtke & Richter, 2007). For this purpose, presentation levels of the stimuli were calibrated using an Artificial Ear (2cc-coupler) connected to a B&K (Brüel & Kjær) 2270 Investigator sound level meter. The reference threshold values (given in dB [peRETSPL]) for each stimulus at the given presentation rate (20

stimuli/s) delivered from the ER-3A insert earphone are shown in table 3-1. Calibration was done by comparing the peak-to-peak value of the acoustic stimulus with that of the reference signal, which was a pure-tone signal corresponding to the center frequency of the octave-band chirp (Figure 2-4). For this purpose, each stimulus was presented in the ER-3A earphone and the electrical output from the artificial ear (2cc-coupler) was stored on the oscilloscope. Then, the corresponding reference pure tone, with frequency equal to the center frequency of the stimulus, was presented in the ER-3A earphone and its level was attuned to get the same peak-to-peak value with the stored one (Fedtke & Hensel, 2010). In this way, the peak-to-peak sound pressure produced in the artificial ear by the chirp stimulus was equal to the peak-to-peak sound pressure of the reference signal with the prescribed peRETSPL (peak-to-peak equivalent Reference Equivalent Threshold Sound Pressure Levels) value. A schematic view of the calibration procedure is shown in Figure 2-5.

Table 2-1: Reference threshold values in dB peETSPL for one octave-band chirps at the repetition rate 20 stimuli/s, using 2cc-coupler presented in the ER-3A (personal communication with Dr. Elberling, 2015).

Octave-band chirp	center frequency of 1000 Hz	center frequency of 4000 Hz
dB peETSPL	18	24.5

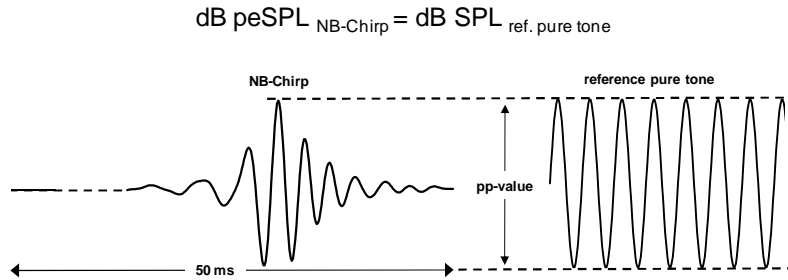


Figure 2-4: Defining the peak-to-peak equivalent Reference Equivalent Threshold Sound Pressure Levels (peRETSPLs). The dB peSPL of each octave-band chirp is equal the sound pressure level (dB SPL) of the sinusoidal signal whose frequency corresponds to the center frequency of the octave-band chirp (Gøtsche-Rasmussen et al., 2012).

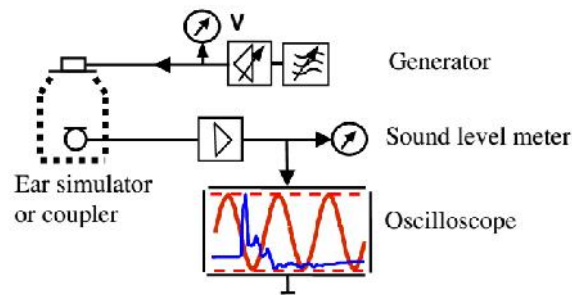


Figure 2-5: A schematic view of measuring the peak-to-peak equivalent Reference Equivalent Threshold Sound Pressure Levels (peRETSPLs) (Fedtke & Hensel, 2010).

Stimuli were presented using a Tucker-Davis Technologies (TDT) RP2.1 Enhanced Real-time Processor controlled by TDT RPvdsEX (v.5.4) software running on a Compaq Evo D51C (Intel P4 @ 2.4 Ghz, 1 GB RAM, Windows XP x86 SP2). TDT software controlled the TDT RP2.1 via a USB interface. Signal output from the TDT RP2.1 was directed through a TDT P5A Programmable Attenuator to create different stimulus presentations levels of 20 dB nHL to 80 dB nHL with 10 dB steps, chosen randomly. Then, the Attenuator output delivered the signal to a

TDT HB7 Headphone Driver (0 dB gain) which drove a single right-channel Etymotic ER-3A (10 Ohm) ear-insert transducer. The delay between the TTL pulse stimulus onsets relative to the actual arrival time of sound at the ear insert was measured and adjusted in order to get accurate timing for recording.

2.4 Psychoacoustic Experiment

In the behavioural task, an instruction was given to each subject (Figure 2-6) indicating that they should rate each sound as one of the six states of “too loud”, “very loud”, “loud”, “OK”, “soft”, “very soft, or indicate “no response” if the stimulus was not heard, by pushing the desired button on the touch screen. The procedure was programmed in Visual Basic. On each trial, one of the 7 intensity levels was chosen randomly and the stimulus was presented for three repetitions. The next trial was presented immediately after the subject had responded to the previous one. This is a quick procedure to measure loudness growth across different frequencies and different levels in both normal and hearing-impaired subjects(Allen, Hall, & Jeng, 1990). The stimuli were the octave-band chirp stimuli described above with center frequencies of 1000 Hz and 4000 Hz and with intensity levels from 20 dB nHL to 80 dB nHL in 10 dB steps.

Each category was defined by a numerical value from 0 to 6, where 0 was assigned to “no response”, 1 to “very soft”, 2 to “soft”, 3 to “OK”, 4 to “loud”, 5 to “very loud” and 6 to “too loud”. These numbers were not known to subjects and were used only for analysis purposes (Allen et al., 1990). The loudness estimation for each specific level was achieved by calculating the geometric mean of subjects’ responses for that level (Silva & Epstein, 2009, 2010, 2012).



Figure 2-6: The behavioral instruction given to each participant to help them to do the task.

2.5 Recording Paradigm of the ABR experiment

Participants were tested individually in a sound-attenuating room (background noise level of 29 dB(A)). During the ABR recording, participants were asked to watch and pay attention to a silent movie (subtitled) and not to the sounds coming from the ear inserts. They were also asked to sit comfortably and minimize their movement, including blinking and facial movements, so as to reduce movement artifacts and obtain the best signal-to-noise ratio in the EEG recording.

Each stimulus was presented for 4000 trials with a repetition rate of 20 stimuli/s, which is the standard repetition rate based on ISO 389-6 2007 (Gøtsche-Rasmussen et al., 2012). Each trial was 50 ms in duration, including a 10 ms chirp stimulus followed by a 40 ms silent inter-stimulus interval (ISI). For the purpose of eliminating the cochlear microphonic which is generated by outer hair cells, from the recording and other interfering artifacts like electromagnetic artifact of the transducer, each stimulus was presented with alternating polarity in blocks of 5 second duration (Elberling and Osterhammel, 1989) and the transducer was

shielded. Stimuli were presented monaurally to the participant's right-ear through a 13 mm disposable adult foam ear-insert tip (ERI-14A; 1.93 mm inside-diameter), which was placed in the participant's right-ear canal for stimulus delivery.

A Compumedics Neuroscan SynAmps RT amplifier (Model: 9032) and Compumedics SCAN 4.5 Acquire software running on an Intel PC (Intel Core i5 @ 3.33 GHz, 4 GB RAM, Windows 7 x64) were used to collect the EEG data. The sampling rate of the recorded voltage from the electrodes was 20 kHz using a 24-bit A/D converter operating in a range of ± 350 mV with 41 nV ($0.700 \text{ V}/224$) least significant bit (LSB) resolution.

Similar to common paradigms for ABR recording, three Ag/AgCl sintered electrodes filled with a conductive gel (Signa Gel) were attached to the head with double-sided tape washers. Electrodes were placed based on the standard ABR vertical montage: an electrode on the center of the forehead was used as a ground and the electrical activity was picked up from electrodes on the vertex (Cz) and the right earlobe (ipsilateral to stimulus delivery). The cranial intersection of the midway point between the ear canals and the midway point between the bridge of the nose and inion was defined as the vertex. The active electrode was connected to a bipolar channel on the SynAmps RT headbox bridged with the reference channel. A software notch filter at 60 Hz and a hardware band-pass filter between 0.5–3000 Hz were applied to the recordings. Furthermore, electrode impedance of the skin and attached electrodes was kept below 15 k Ω for all subjects.

2.6 Estimation of Loudness Growth from Evoked ABRs and Psychoacoustic Procedure

The estimation of loudness growth at each intensity level, from the psychoacoustical procedure was calculated as the geometric mean of the non-zero numbers of participants'

responses. Results obtained for each category of loudness scaling as a function of stimulus intensity have been shown in the next chapter.

The recorded chirp evoked ABR signals at each intensity level were filtered using a band-passed filter from 100 Hz to 3000 Hz with a slope of 12 dB/Octave. A six-order Butterworth infinite impulse response filter was designed in MATLAB and applied off-line in conjunction with the function of `FILTFILT` in order to ensure that the filtered response had no phase shifts. Afterwards, an artifact rejection threshold of 50 microvolt was used to eliminate trials with excessive noise for the next steps of the analysis. Then, the preprocessed signals of both polarities at each level were averaged using the modified weighted averaging method of Epstein & Silva (2009) which was explained in section 2.3.2. In each recorded evoked ABR the salient response peak wave V was identified and the peak-to-trough amplitude (Elberling et al., 2010) was measured as a physiological feature of the loudness estimation at each intensity level (dB nHL). Then two curve fittings, linear and power, were chosen to establish the relationship between the psychacoustical loudness estimation and the estimated one from the ABRs of each participant. The model that provided the best fit for each stimulus was identified by comparing the adjusted R-squared values of each curve fitting across all the participants. Finally, the estimated loudness as a function of stimulus intensity obtained from the best models, were compared with equal-loudness contours and the estimated loudness from the loudness model for time-varying sounds (Glasberg, & Moore, 2002).

3. Results

In this chapter, the results from the subjective psychacoustical procedure and the measured amplitude of ABR wave V are presented. In order to investigate the relation between the psychacoustical results and amplitude of wave V (peak-to-trough amplitude), visual inspection was used initially to determine the functions that would best fit the data. Two functions were selected and compared as reported in the following section.

3.1 Psychoacoustical Results

As described in the previous chapter, the same stimuli were used in both the psychoacoustical and ABR procedures. In the subjective psychoacoustical task, each participant was asked to rate the loudness of each stimulus in seven categories (as shown in Figure 3-6), where each stimulus was presented three times. The stimulus levels (presented in dB nHL) of each rated category from ‘very soft’ to ‘too loud’ were averaged across the subjects. There were no significant differences between the results from the two one-octave band chirp stimuli with center frequencies of 1000 Hz and 4000 Hz; therefore, the data were pooled and averaged over frequencies to give the normative reference for the psychoacoustic task. The calculated chirp-stimulus level for each category are shown in the first row of Table 3-1.

Table 3-1: The normative reference data corresponding to the common categories very soft, soft, comfortable, loud, very loud, and too loud from one-octave band chirp stimuli (this study) and the seven procedures presented in (Elberling, 1999) in dB HL.

Loudness rating	Too loud	Very loud	Loud	Ok	Soft	Very soft
Chirp Stimuli	---	80	75.1	64.85	45.55	26.2
Kiessling, Schubert, & Wagner, 1994	92.5	87.5	75	64	48.8	22.5
Hohman, & Kollmeier, 1995	106.3	99.3	85.2	71.1	57	42.9
Launer, 1995	112.7	103.4	84.9	66.4	47.2	29.4
Ricketts & Bentler, 1996	-----	-----	81.8	62.9	35.5	20.5
Allen et al., 1990	102.6	97.6	90.2	78.6	58.9	34.4
Elberling, & Nielsen, 1993	125.3	115.6	103.8	89.1	69.3	39.4
Cox, Alexander, Taylor, & Gray, 1997	101	-----	91.9	67.0	39.3	20.3

Table 3-1 shows the sound level (dB nHL) corresponding to each category from ratings of subjects with normal hearing from several published studies. Although all studies used narrowband stimuli and had the same loudness categories, there are some differences in the ratings across studies. Some factors, such as stimulus parameters (e.g., type and bandwidth of the stimulus), presentation parameters (e.g., randomization, stimulus frequency), instructions to the test subjects (e.g., number of categories), and so on, may be related to these differences. Table 3-2 shows the stimulus type used in each procedure.

Table 3-2: Stimulus type in each loudness scaling psychoacoustic task.

Study	Type	Level presentation
Present study	One-octave band chirp	random
Kiessling et al., 1994	1/3-octave filtered noise	random
Hohman, & Kollmeier, 1995	1/3-octave filtered noise	random
Launer, 1995	one critical band "frozen" noise	random
Ricketts & Bentler, 1996	1/3-octave noise	random
Allen et al., 1990	½-octave band of wide noise	random
Elberling, & Nielsen, 1993	pure-tone	random
Cox et al., 1997	warble tone	ascending level

Figure 3-1 shows the corresponding loudness scaling of each psychoacoustic procedure as a function of stimuli level. A power-law function has been fitted to each data set and reported in Table 3-3. The average power-law exponent of the listed published studies is 1.35 which is very close to the calculated power-law exponent of 1.36 found in the present study, obtained from one-octave band chirp stimuli.

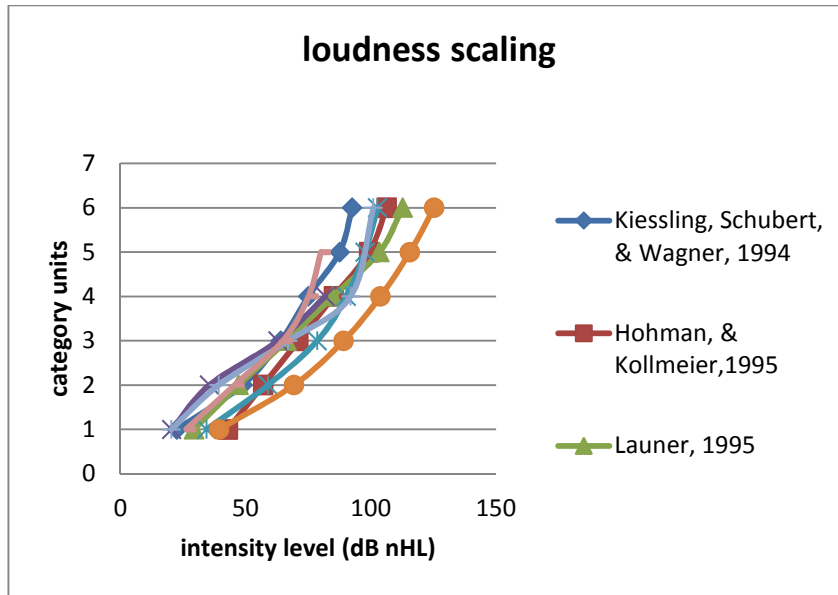


Figure 3-1: The normative reference (i.e., categories versus sound level (dB nHL)) for data from seven published loudness scaling procedures and the present study. Each category unit shows a specific loudness scale (i.e., 0 assigned to ‘not heard’, 1 assigned to ‘very soft’, 2 assigned to ‘soft’, 3 assigned to ‘OK-comfortable’, 4 assigned to ‘loud’, 5 assigned to ‘very loud’ and 6 assigned to ‘too loud’).

Table 3-3: Power-law exponent of the curve-fitting for each psychoacoustic method.

	Chirp Stimuli	Kiessling et al., 1994	Hohman, & Kollmeier, 1995	Launer, 1995	Ricketts & Bentler, 1996	Allen et al., 1990	Elberling, & Nielsen, 1993	Cox et al., 1997
Power-law exponent	1.36	1.23	1.89	1.28	0.96	1.57	1.53	1.01
R-squared	0.98	0.96	0.99	0.99	0.98	0.97	0.98	0.96

3.2 Chirp Evoked ABR Results

As explained in the previous chapter, auditory brainstem responses to two octave-band chirp stimuli with center frequencies of 1000 Hz and 4000 Hz were recorded at different intensities from 20 dB nHL to 80 dB nHL in 10 dB steps. The number of recorded trials for each

intensity level was 4000, half with inverse polarity. After pre-processing the recorded trials, weighted averaging based on Bayesian inference was done and the absolute amplitude of the most salient response peak, wave V, was measured for each averaged signal at each specific intensity level. The data in each condition are described by the sample mean and standard deviation across all the subjects, as shown in Tables 3-4 and 3-5 for chirp stimuli with center frequencies of 1000 Hz and 4000 Hz respectively. In general, the amplitudes of the ABR components increased as stimulus intensity increased and yielded positive power functions with R-squared values of 96% and 98%, respectively (Figure 3-2).

Table 3- 4: Average and standard deviations of measured amplitude of wave V across all the participants. Evoked ABR was obtained by presenting the one octave-band chirp stimulus with 1000 Hz center frequency.

Level(dB nHL)	20	30	40	50	60	70	80
Mean (microvolt)	0.24625	0.265	0.34125	0.36875	0.46	0.5025	0.50125
Std.	0.059207	0.105684	0.096963	0.108108	0.193203	0.131895	0.131059

Table 3-5: Average and standard deviations of measured amplitude (microvolt) of wave V across all the participants. Evoked ABR was obtained by presenting the one octave-band chirp stimulus with 4000 Hz center frequency.

Level(dB nHL)	20	30	40	50	60	70	80
Mean (microvolt)	0.244545	0.282727	0.306364	0.358182	0.377273	0.387273	0.437273
Std.	0.082263	0.117991	0.080284	0.130293	0.085451	0.093605	0.125466

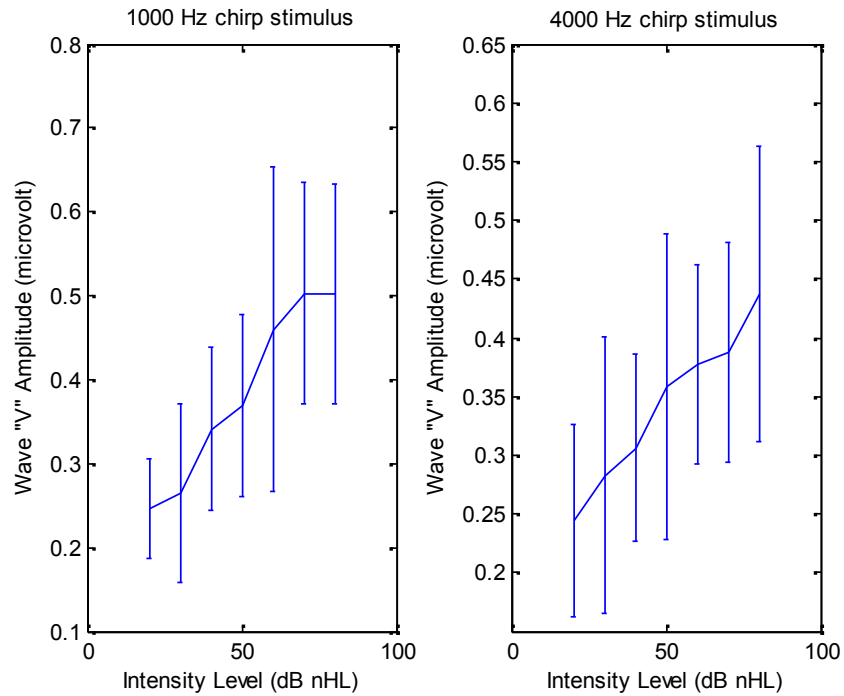


Figure 3-2: The averaged wave V amplitude data (across subjects) and standard deviation as a function of stimuli intensity (dB nHL). The left plot corresponds to obtained data from evoked ABRs to one-octave band chirp stimulus with center frequency of 1000 Hz and the right plot shows that of evoked ABRs to one-octave band chirp stimulus with center frequency of 4000 Hz.

3.3 Estimation of Individual Loudness Growth through Evoked ABR

The loudness growth at each level was estimated by the geometric mean of the non-zero numbers (assigned to each category) of participants' ratings from the psychoacoustical procedure. Loudness growth was also estimated from physiological data, specifically, the wave V amplitude of the averaged ABR at each intensity level. In order to investigate the feasibility of using ABR as an objective measure for loudness growth estimation, two functions, linear and power-law functions, were used to examine the relationship between predictor (wave V amplitude) and response (psychoacoustic measure) variables. In order to improve the curve fitting, weighted fitting was done in which less weight was given to less precise measurements

and more weight to more precise measurements. Specifically, applied weights were defined to be inversely proportional to the calculated variance at each level obtained from the modified method of Silva (2009) described in Section 2.3.2. Linear and power curve fittings are compared in Section 4.3.3.

3.3.1 Linear Function Fitting

Tables 3-6 and 3-7 show the descriptive measure of goodness of fit of the linear trend (R-squared values) for each individual in response to the one octave-band chirp stimuli with center frequencies of 1000 Hz and 4000 Hz, respectively. R-squared values corresponding to the weighted linear fitting has been reported as well. Although the R-squared value is higher on average in the weighted than non-weighted case, the difference was not statistically significant by a t-test ($p = 0.6$ for both the 1000 Hz and the 4000 Hz stimuli). Figures 3-3 and 3-4 show the parameters of the linear function fitting using data obtained from all the participants. The group R-square value for each of the two chirp stimuli is lower than the average of the R-square values of individuals, which indicates that there are differences among participants.

Table 3-6: R-squared values for linear fitting between psychoacoustic and ABR estimates of loudness growth for each individual participant with one octave-band chirp stimulus with center frequency of 1000 Hz. The first column shows the ordinary fitting and second column shows the linear weighted fitting.

Subject	Unweighted fit	Weighted fit
S1	0.6181	0.7169
S2	0.591	0.5971
S3	0.4324	0.347
S4	0.2753	0.3279
S5	0.7233	0.7359
S6	0.295	0.2819
S7	0.8227	0.8063
S8	0.7002	0.7376
S9	0.5266	0.7494
S10	0.5262	0.3443
S11	0.8264	0.8498
Mean	0.576109	0.590373
Std.	0.189104	0.219535

Table 3-7: R-squared values for linear fitting between psychoacoustic and ABR estimates of loudness growth for each individual participant with one octave-band chirp stimulus with center frequency of 4000 Hz. The first column shows the ordinary fitting and second column shows the linear weighted fitting.

Subject	Unweighted fit	Weighted fit
S1	0.1135	0.1072
S2	0.2822	0.2897
S3	0.3239	0.4482
S4	0.003533	0.008679
S5	0.719	0.7087
S6	0.5168	0.5491
S7	0.3466	0.384
S8	0.7731	0.7702
S9	0.6863	0.5962
S10	0.83	0.8364
S11	0.5333	0.5099
Mean	0.466203	0.47348
Std.	0.274376	0.262642

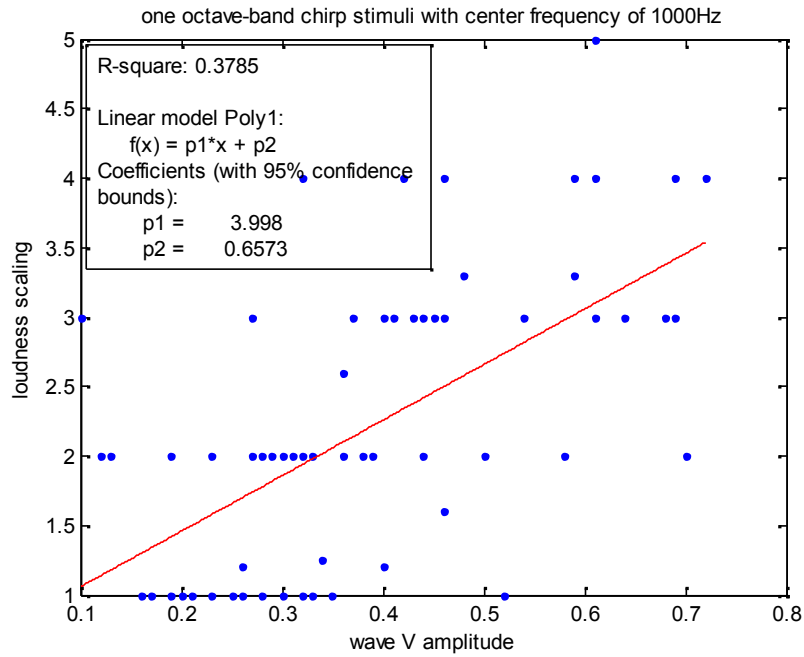


Figure 3-3: Linear fitting using data of all the participants with one octave-band chirp stimulus with 1000 Hz center frequency.

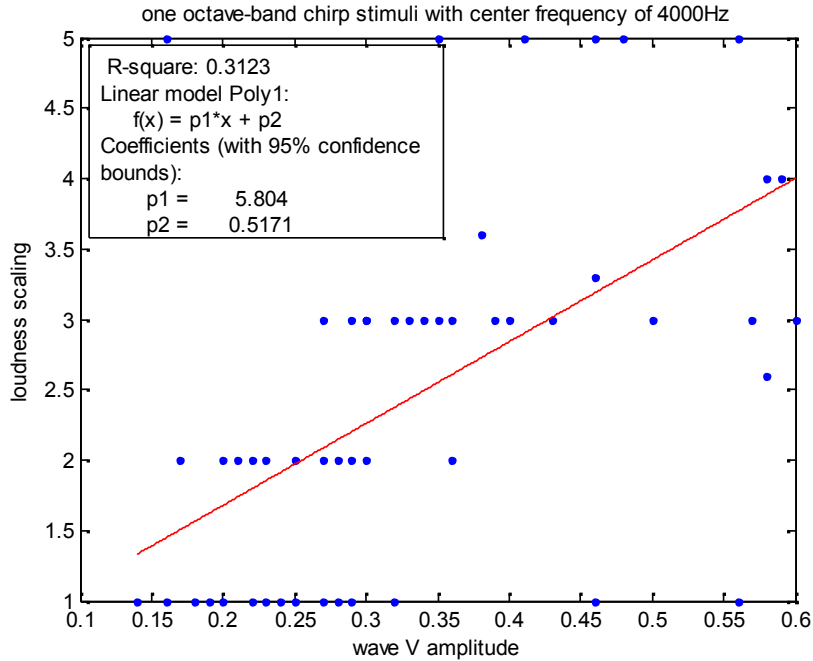


Figure 3-4: Linear function fitting using data of all the participants with one octave-band chirp stimulus with 4000 Hz center frequency.

3.3.2 Fitting Power function

The procedures of the previous Section were repeated using a power function. The R-square values for both normal and weighted fittings are reported in Tables 3-8 and 3-9, which show a small, although non-significant ($p = 0.9$ for the 1000 Hz stimulus and $p=0.6$ for the 4000 Hz stimulus), advantage of using the weighted over non-weighted power function fitting. The averaged R-square value of individual data obtained from the 1000 Hz chirp stimulus is 0.68 and that from the 4000 Hz stimuli is 0.53. The power function fitting on pooled data obtained from all subjects is shown in Figures 3-5 and 3-6, which again shows lower R-square values in comparison with averaged R-square values across subjects.

Table 3-8: R-squared values for the power function fitting between psychoacoustic and ABR estimates of loudness growth for each individual participant with the one octave-band chirp stimulus with center frequency of 1000 Hz. The first column shows the ordinary fitting and the second column shows the power function weighted fitting.

Subject	Unweighted fit	Weighted fit
S1	0.6791	0.7597
S2	0.8628	0.8635
S3	0.5398	0.478
S4	0.3818	0.4182
S5	0.7325	0.7459
S6	0.519	0.509
S7	0.8325	0.809
S8	0.7492	0.7731
S9	0.8201	0.8986
S10	0.5871	0.4447
S11	0.8499	0.8634
Mean	0.686709	0.687555
Std.	0.159796	0.185586

Table 3-9: R-squared for power function fitting between psychoacoustic and ABR estimates of loudness growth for each individual participant for the one octave-band chirp stimulus with center frequency of 4000 Hz. The first column shows the ordinary fitting and the second column shows the power function weighted fitting.

Subject	Unweighted fit	Weighted fit
S1	0.2311	0.2631
S2	0.292	0.297
S3	0.3257	0.4516
S4	0.02666	0.02919
S5	0.7227	0.7194
S6	0.6392	0.6634
S7	0.412	0.4527
S8	0.828	0.8294
S9	0.8009	0.6654
S10	0.8803	0.8725
S11	0.5695	0.5898
Mean	0.520733	0.530317
Std.	0.280993	0.259033

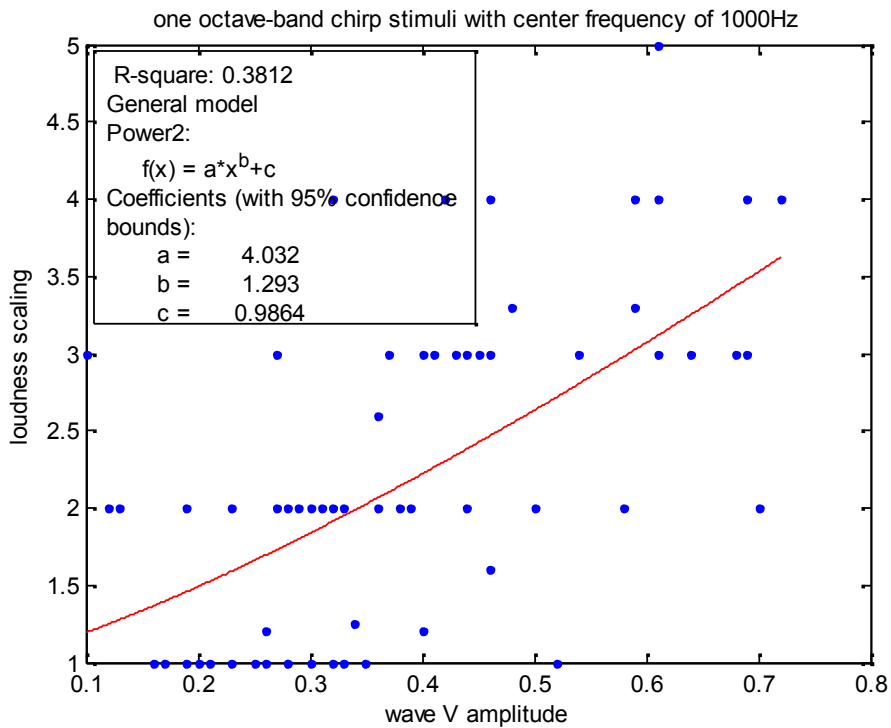


Figure 3-5: Power-law function fitting using data from all participants with the one octave-band chirp stimulus with 1000 Hz center frequency.

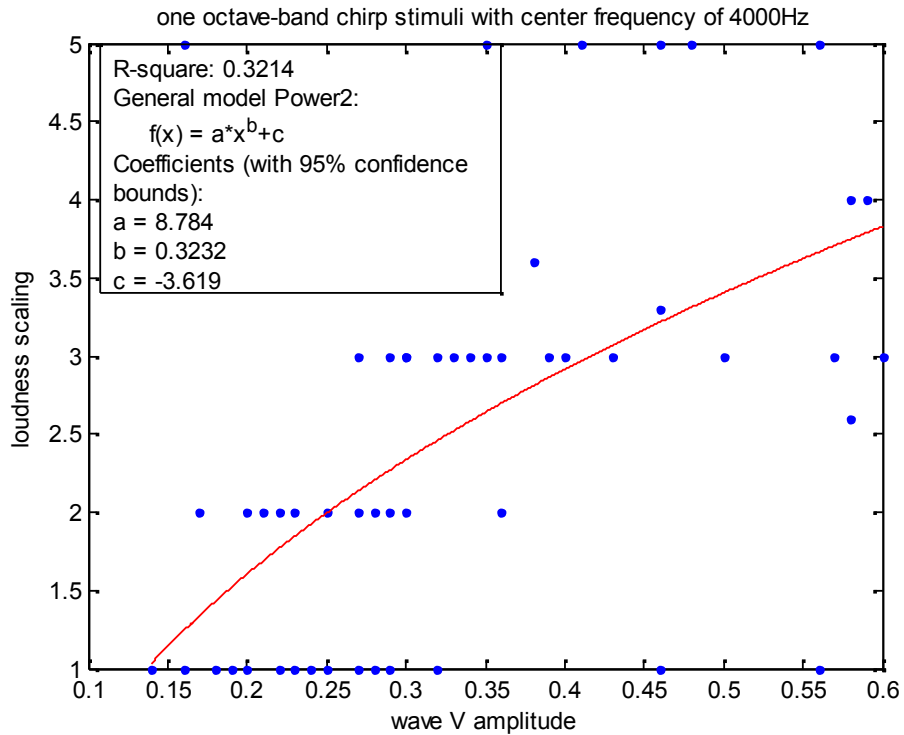


Figure 3-6: Power-law function fitting using data from all the participants with the one octave-band chirp stimulus with 4000 Hz center frequency.

3.3.3 Comparison between Linear and Power Function Fitting

In order to compare the goodness of fit of the two models, it is important to consider differences between the two selected functions in the number of predictors. The linear function has two coefficients while the power function used in this study has three coefficients (Equations 4-1 and 4-2). Therefore, in order to compare the efficiency of each model, adjusted R-squared values were used. The adjusted R-squared value is the modified version of R-squared that takes into account the number of coefficients and predictors in the model. If the new added term to the given function improves the fitness beyond what would be expected from adding an extra degree of freedom, the adjusted R-squared increases fit, otherwise it decreases. The adjusted R-squared

values of each individual are reported in Tables 3-10 and 4-11, showing the results of data obtained from the 1000 Hz and 4000 Hz chirp stimuli, respectively. Because the weighted fittings were somewhat better than the ordinary fittings, in this Section only the adjusted R-squared values of the weighted fittings of two functions were compared.

$$f(x) = ax + b \quad \text{linear model} \quad (3 - 1)$$

$$f(x) = ax^b + c \quad \text{power model} \quad (3 - 2)$$

Table 3-10: Adjusted R-squared values for each individual for the two weighted fitting functions, linear and power for the one octave-band chirp stimulus with center frequency of 1000 Hz.

Subject	Linear fit (weighted)	Power fit (weighted)
S1	0.6602	0.6396
S2	0.5165	0.7953
S3	0.2164	0.217
S4	0.1935	0.1273
S5	0.6799	0.6139
S6	0.1382	0.2635
S7	0.7675	0.7135
S8	0.6852	0.6597
S9	0.6993	0.8479
S10	0.2131	0.167
S11	0.8197	0.7951
Mean	0.508136	0.530891
Std.	0.263237	0.278242

Table 3-11: Adjusted R-squared values for each individual for the two weighted fitting functions, linear and power for the one octave-band chirp stimulus with center frequency of 4000 Hz.

Subject	Linear fit (weighted)	Power fit (weighted)
S1	-0.07137	-0.1054
S2	0.1387	-0.06199
S3	0.3379	0.1773
S4	-0.1896	-0.4607
S5	0.6504	0.579
S6	0.4589	0.4952
S7	0.2608	0.179
S8	0.7242	0.7441
S9	0.5155	0.4981
S10	0.8036	0.8087
S11	0.4118	0.3548
Mean	0.391073	0.34311
Std.	0.275369	0.305693

The adjusted R-squared values for linear and power functions were not significantly different for both the 1000 Hz stimulus and the 4000 Hz stimulus (p-value = 0.8 for the 1000 Hz stimulus and p-value= 0.7 for the 4000 Hz stimulus). Thus, the linear fit was chosen as it has fewer parameters. This suggests that the relation between the psychoacoustically determined loudness of growth and the estimate from the wave V amplitude of recorded ABR can be characterized fairly well by a linear function.

4. Discussion

The results from the adjusted R-squared values of the linear and power fitted functions on the obtained data from the psychoacoustic task and the measured wave V amplitude showed that there is no significant advantage for the power function over the linear function. The significant linear relationship between the obtained data of two tasks at different intensity levels indicates that the ABR may be a good way to assess the loudness growth function objectively.

However, as shown in figure 4-1, there is large individual variability among participants. For some participants there is a very good linear relationship between wave V amplitude and the scaled loudness (R-squared values of up to 0.8), which shows the potential of using this procedure for loudness growth evaluation. However, for other participants, the R-squared value was close to zero. Figures 4-2 and 4-3 show the loudness scaling obtained from the psychoacoustic task as a function of measured wave V amplitude for the best and the worst subject at each frequency. The reason for the lack of correspondence between the two procedures for some participants is difficult to determine. While the ABR response may not have been a good indication of growth of loudness in some participants, it is also possible that it was the psychoacoustic measure that was not accurate. For example, some subjects may not have attended adequately in making their judgements during the psychoacoustic task and may have found it difficult to maintain consistent ratings on the 7-point scale. Besides these limitations, it is obvious that fitting a perfect line on the discrete values of loudness rate obtained from the psychoacoustic task as a function of continuous values of the ABR wave V amplitude, is impossible. Therefore, it would be worth duplicating the project with other psychoacoustic methods with continuous scaling for loudness rating.

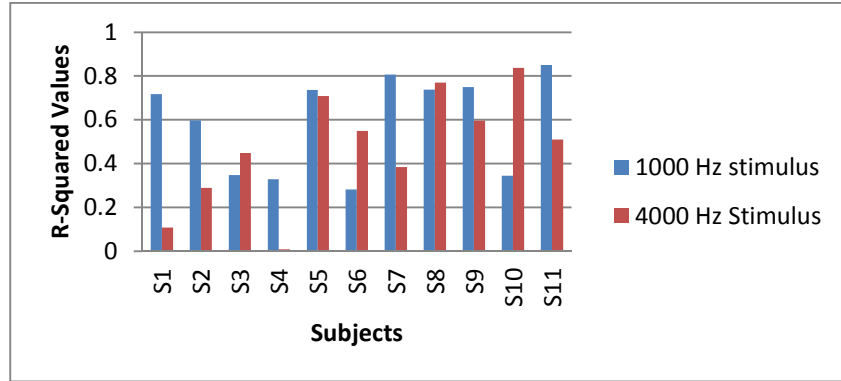


Figure 4-1 Relationship between R-Squared values (linear fit between psychoacoustic data and wave V amplitude) for each subject at 1000 and 4000 Hz.

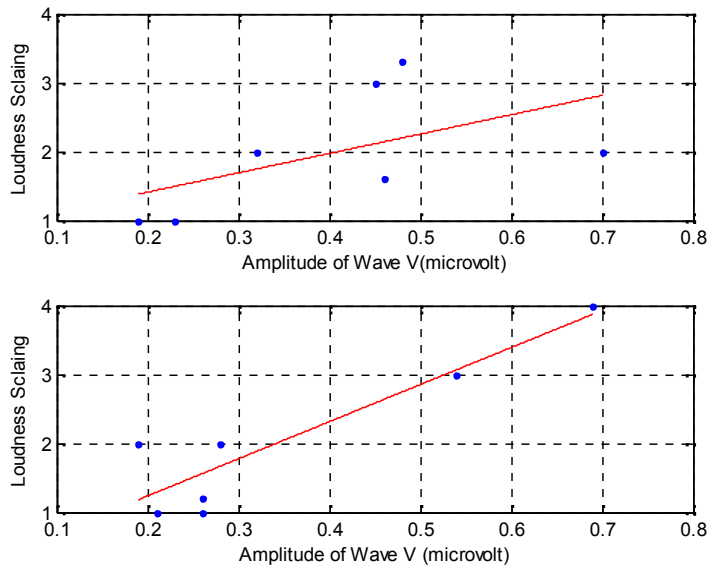


Figure 4-2: Comparison between psychoacoustic and ABR data for the two individuals with the worst (upper plot) and the best (lower plot) linear fit for the 1000 Hz chirp stimulus.

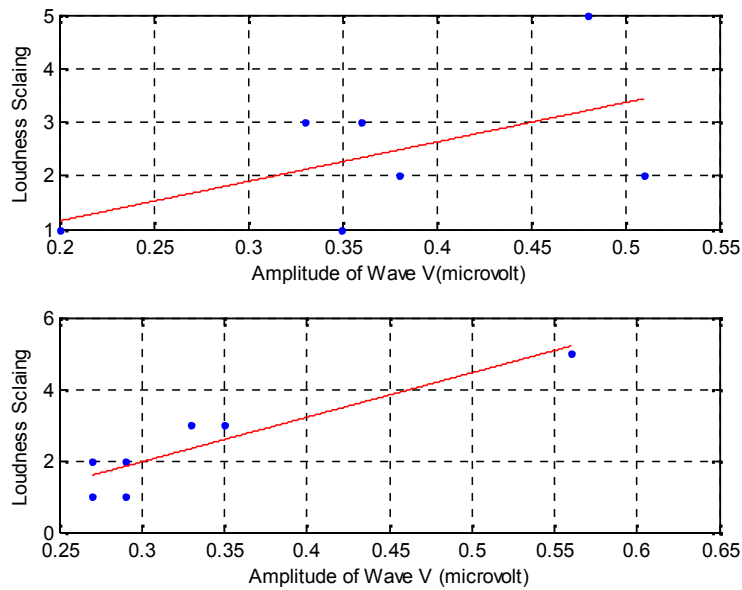


Figure 4-3: Comparison between psychoacoustic and ABR data for the two individuals with the worst (upper plot) and the best (lower plot) linear fit for the 4000 Hz chirp stimulus.

Previous studies mostly used click stimuli-evoked ABRs for loudness growth evaluations (e.g. Davidson, Wall, & Goodman, 1990; Gallego et al., 1996; Gallégo et al., 1999; Serpanos, O'Malley, & Gravel, 1997; Wilson & Stelmack, 1982). The problem with this approach is that the click evoked ABR is not frequency specific. Only one other study has tried to evaluate loudness growth with ABR using frequency specific stimuli, and this study used tone bursts (Silva & Epstein, 2010). Although they concluded that loudness-growth estimation obtained through tone-burst evoked ABR is comparable with psychoacoustical results, the chirp stimuli from the present study offer the advantage over the Silva & Epstein (2010) study that many fewer trials are needed. Silva & Epstein (2010) recorded 12000 trials for each condition while in the present study, only 4000 trials were recorded. The shorter time required and a greater confidence in the interpretation of the ABRs with chirp stimuli (e.g. Dau et al., 2000; Elberling et al., 2010, 2007; Elberling & Don, 2007, 2008, 2010; Ferm, Lightfoot, & Stevens, 2013; Fobel &

Dau, 2004; Gøtsche-Rasmussen, Poulsen, & Elberling, 2012; Maloff & Hood, 2014; Ribeiro, Rodrigues, & Lewis, 2012; Rodrigues, Ramos, & Lewis, 2013; Stuart & Cobb, 2014) make it a more promising procedure for evaluating loudness growth in clinics.

Many factors affect the estimated loudness from both psychoacoustic and objective methods, such as stimulus duration and stimulus frequency (Elberling, 1999). In order to compare the loudness of each applied stimulus with its specific frequency at each intensity level, the estimated loudness using the two obtained models of the previous chapter were compared to two different models of loudness, equal loudness contours and the loudness model for time-varying sounds (Glasberg, & Moore, 2002). Based on linear function fitting results, suppose that the linear functions which have been shown in Figure 3-5 and Figure 3-4 were defined as a model for 1000 Hz octave-band chirp stimulus and 4000 Hz octave-band chirp stimulus, respectively:

$$f(x) = 3.9998x + 0.6573 \quad \text{linear model for 1000 Hz chirp stimulus (4 – 3)}$$

$$f(x) = 5.804x + 0.5171 \quad \text{linear model for 4000 Hz chirp stimulus (4 – 4)}$$

where $f(x)$ shows the predicted loudness scaling for the measured amplitude of wave V, x , at each level of the recorded ABR.

Therefore, it is obvious (Figure 4-3) that for a given range of amplitudes of wave V (e.g., 0.2 microvolt to 0.7 microvolt), the predicted loudness scale, for each specific amplitude value of the 4000 Hz chirp stimulus, is higher than that of the 1000 Hz chirp stimulus. Given that the amplitude of wave V increases as stimulus intensity increases, we can conclude that for the same stimulus intensity, our model predicts a higher perceived loudness for the stimulus with center frequency of 4000 Hz compared to that of the stimulus with center frequency of 1000 Hz.

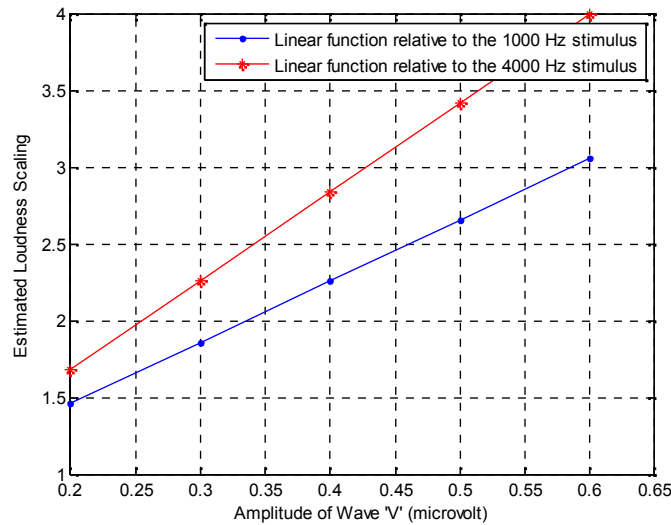


Figure 4-4: Estimated loudness scale at each amplitude of wave V for linear obtained models. The blue line is relative to the obtained linear models for the 1000 Hz chirp stimulus. The red line shows the linear model obtained for the 4000 Hz chirp stimulus.

This conclusion is in agreement with Figure 4-5, which shows that the loudness of a 4000 Hz stimulus is perceived as higher than that of a 1000 Hz stimulus (when they are presented at the same intensity level). However, the equal-loudness contours presented in Figure 4-4 were measured in free sound fields with pure tones. Therefore, the dip around the 4000 Hz region with equal-loudness contours might be caused by pinna and ear canal effects on the mid frequencies from 2000 Hz to 7000 Hz. Given that the data presented here were obtained through ear insert stimulus presentation, the greater perceived loudness at 4000 Hz seen in the presence study cannot be caused by pinna effects.

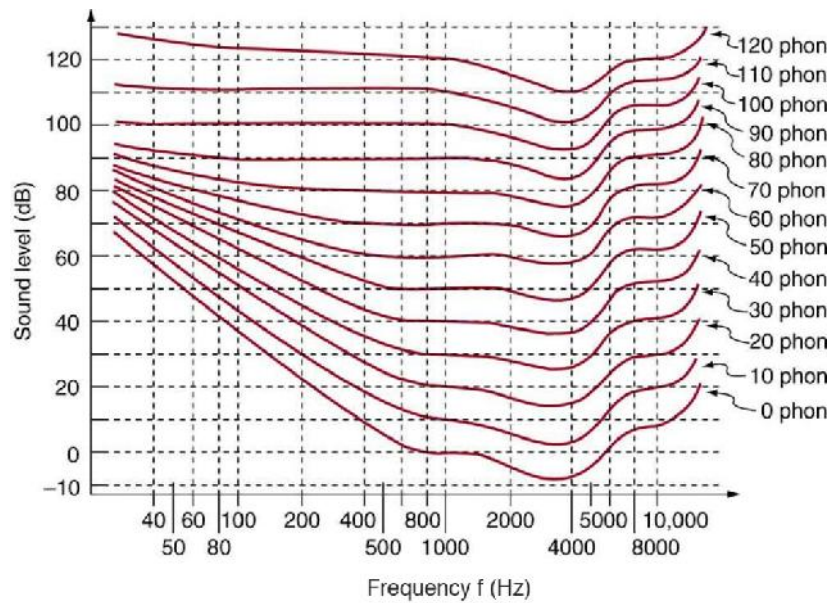


Figure 4-5: The relationship of loudness in phons to intensity level (in decibels) for normal hearing people. The curved lines are equal-loudness curves (Metabolic, 2012).

Another model worth considering is the loudness model for time-varying sounds (Glasberg, & Moore, 2002) which used data measured with in-the-ear microphones, similar to our procedure. The estimated loudness according to this model for the two stimuli with center frequencies of 1000 Hz and 4000 Hz are plotted across intensity in dB nHL in Figure 4-6. It is obvious from Figure 4-6, that the estimated loudness for the 4000 Hz stimulus is higher than that obtained for the 1000 Hz stimulus when at lower intensities, which is in agreement with results of present study. However, the estimated loudnesses obtained by this model are similar for both frequencies at higher intensities, unlike the data in the present study. The model of Glasberg, & Moore (2002) used binaural conditions while our experiments were done monaurally, so this may explain the differences. It is well documented that a tone presented binaurally through earphones is perceived as louder than the same stimulus presented monaurally (Fletcher & Munson, 1933). This phenomenon is called binaural loudness summation and although almost no dependence of

this phenomenon on stimulus frequency has been reported (Zhang & Mao, 2010), this phenomenon may explain the lower perceived loudness of 4000 Hz at higher stimulus levels in the loudness model of Glasberg, & Moore (2002) compared to obtained results in this thesis. Furthermore, the model of Glasberg, & Moore (2002) has been designed for stimulus with larger duration than the stimulus used in this study, which may be the other reason of different perceived loudness at higher stimulus intensities. On the other hand, fitted lines on the loudness results obtained from the psychoacoustic tasks (Figure 4-7) are in agreement with loudness estimations of the obtained models (Figure 4-3), while they are not in agreement with the Moore model. It is hard to tell if the obtained psychoacoustic data are not accurate or the loudness model of Glasberg, & Moore (2002) does not work for loudness estimation in the stimulus conditions used in the present study. Clearly, further investigation is required, but to the author's knowledge, no report of evaluating loudness growth using the chirp stimulus in monaural conditions exists to compare with obtained results of the present study. Increasing the number of subjects would help to obtain more precise results from both tasks. It would be also worthwhile to do the procedure with higher intensity levels to check if estimated loudness from our models converges at higher intensity levels.

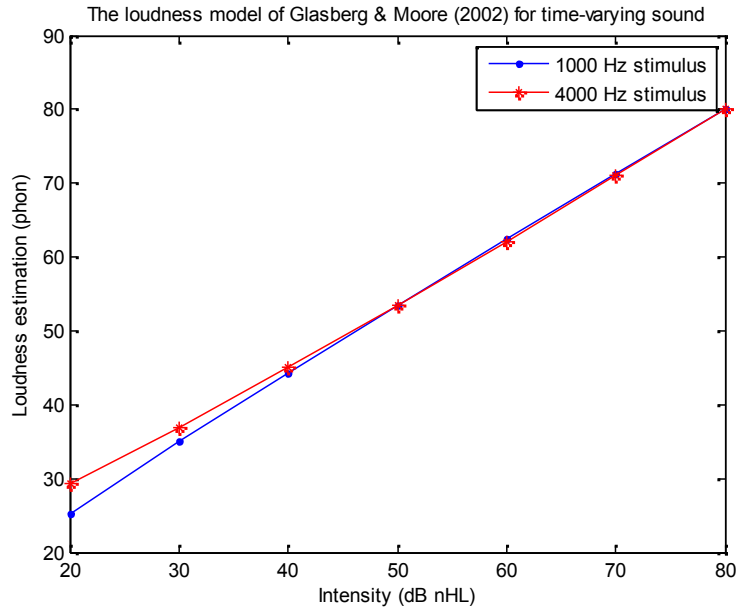


Figure 4-6: Estimated loudness (phon) based on the model of Glasberg, & Moore (2002) for two different stimuli presented at the same intensity levels (dB nHL).

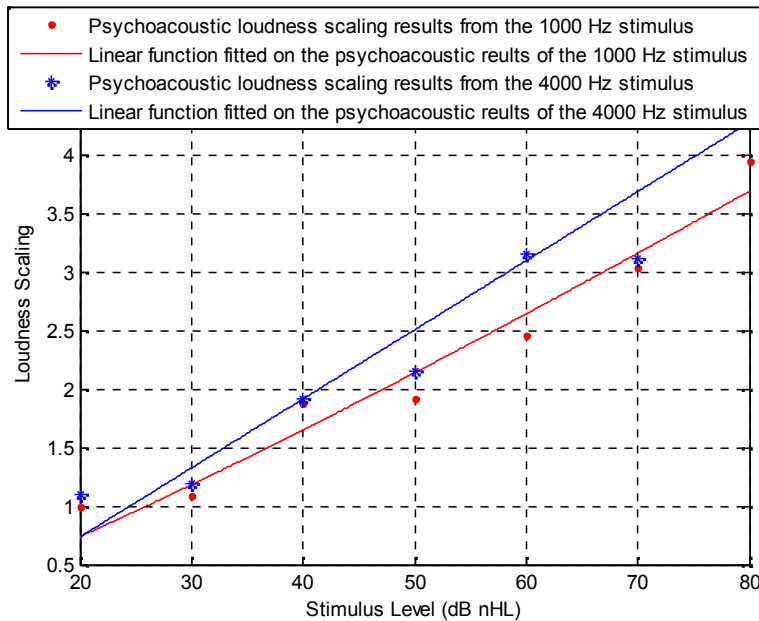


Figure 4-7: Linear function fitted on the obtained loudness scales from the psychoacoustic tasks as a function of stimulus level (in dB nHL). The blue line is relative to the obtained linear fit for the 4000 Hz chirp stimulus. The red line shows the linear fit obtained for the 1000 Hz chirp stimulus.

5. Summary and Conclusion

Considering the disadvantages of using subjective psychoacoustic methods in assessing loudness growth in the clinic, such as bias, inconsistent perceptual judgments across the test sessions, sustained attention, and ability to make a conscious judgement, it is important to investigate the use of objective methods to evaluate the loudness growth for hearing aid fitting. Here we compared psychoacoustic and ABR procedures. Furthermore, octave band chirp stimuli were used, which have advantages over click and tone burst stimuli, such as yielding a higher signal to noise ratio and larger wave V amplitude in the ABR, which leads to easier and more confident interpretation of the ABR as well as to shorter testing time.

Furthermore, instead of using normal averaging methods that are the most common ways of improving signal to noise ratio, a modified version of weighted averaging, which accounted for the non-stationary background noise by assuming multiple discrete locally stationary noise sources, was done on the recorded chirp evoked ABRs. The amplitude of the most salient wave of the evoked ABR, wave V, was measured and two functions, linear and power functions, were applied to examine the relationship between wave V of the recorded ABR and the subjective loudness rating of each individual.

The psychoacoustic results were in good agreement with other studies that applied the same procedure of loudness scaling to assess the loudness growth functions with normal hearing people. Furthermore, the strong linear relationship found between the psychoacoustic results and the physiological results for many subjects shows that despite some limitations, this procedure is reasonably promising. Actually, the poor correspondence between the psychoacoustic and physiological results in a few participants might have been caused by poor compliance on the psychoacoustics test and not necessarily the result of the ABR measure.

In the future, it would be worthwhile to increase the number of participants and to use a different range of frequencies and intensity levels to obtain more comprehensive results. Moreover, increasing the number of recorded trials may improve the signal to noise ratio, leading to more reliable responses. It would also be of interest to compare ABR results to different psychoacoustic methods for measuring loudness growth. In particular, a continuous rating scale, rather than the discrete one used here, has the potential to increase the significance of the fit between the ABR measure and the behavioural psychoacoustic measure. It will also be necessary to test populations with hearing loss. Most importantly, considering the advantages of using chirp stimuli and the growing popularity of using chirp stimuli in audiology clinics compared to click and tone burst stimuli, more studies evaluating loudness growth with both psychoacoustic methods and objective methods using such stimuli would be valuable.

Reference:

- Allen, J. B., Hall, J. L., & Jeng, P. S. (1990). Loudness growth in 1/2-octave bands (LGOB)--a procedure for the assessment of loudness. *The Journal of the Acoustical Society of America*, 88(2), 745–753. <http://doi.org/10.1121/1.399778>
- Buus, S., & Florentine, M. (2001). Modifications to the power function for loudness. *Fechner Day*, 236–241.
- Buus, S., Florentine, M., & Poulsen, T. (1997). Temporal integration of loudness, loudness discrimination, and the form of the loudness function. *The Journal of the Acoustical Society of America*, 101(2), 669–680. <http://doi.org/10.1121/1.417959>
- Coats, a C., & Martin, J. L. (1977). Human auditory nerve action potentials and brain stem evoked responses: effects of audiogram shape and lesion location. *Archives of Otolaryngology*, 103(10), 605–622. <http://doi.org/10.1001/archotol.1977.00780270073012>
- Cox, R. M., Alexander, G. C., Taylor, I. M., & Gray, G. a. (1997). The contour test of loudness perception. *Ear and Hearing*, 18(5), 388–400. <http://doi.org/10.1097/00003446-199710000-00004>
- Dau, T., Wegner, O., Mellert, V., & Kollmeier, B. (2000). Auditory brainstem responses with optimized chirp signals compensating basilar-membrane dispersion. *The Journal of the Acoustical Society of America*, 107(3), 1530–1540. <http://doi.org/10.1121/1.428438>
- Davidson, S. a, Wall, L. G., & Goodman, C. M. (1990). Preliminary studies on the use of an ABR amplitude projection procedure for hearing aid selection. *Ear and Hearing*, 11(5), 332–339. <http://doi.org/10.1097/00003446-199010000-00003>
- Davidson, S. A., Wall, L. G., & Goodman, C. M. (1990). Preliminary studies on the use of an ABR amplitude projection procedure for hearing aid selection. *Ear and Hearing*, 11(5), 332–339. <http://doi.org/10.1097/00003446-199010000-00003>
- De Boer, E. (1980). Auditory physics. Physical principles in hearing theory. I. *Physics Reports*, 62(2), 87–174. [http://doi.org/10.1016/0370-1573\(80\)90100-3](http://doi.org/10.1016/0370-1573(80)90100-3)
- De Boer, E. (1991). Auditory physics. Physical principles in hearing theory. III. *Physics Reports*, 203(3), 125–231. [http://doi.org/10.1016/0370-1573\(91\)90068-W](http://doi.org/10.1016/0370-1573(91)90068-W)
- Don, M., & Elberling, C. (1994). Evaluating residual background noise in human auditory brainstem responses. *The Journal of the Acoustical Society of America*, 96(5 Pt 1), 2746–2757.
- Don, M., Kwong, B., & Tanaka, C. (2005). A diagnostic test for Ménière's Disease and Cochlear Hydrops: impaired high-pass noise masking of auditory brainstem responses. *Otology & Neurotology : Official Publication of the American Otological Society, American*

Neurotology Society [and] European Academy of Otolology and Neurotology, 26(4), 711–722. <http://doi.org/10.1097/01.mao.0000169042.25734.97>

Don, M., Ponton, C. W., Eggermont, J. J., & Masuda, a. (1994). Auditory brainstem response (ABR) peak amplitude variability reflects individual differences in cochlear response times. *The Journal of the Acoustical Society of America*, 96(6), 3476–3491. <http://doi.org/10.1121/1.410608>

Eggermont, J. J. (1979). Narrow-band AP latencies in normal and recruiting human ears. *The Journal of the Acoustical Society of America*, 65(2), 463–470. <http://doi.org/10.1121/1.382345>

Eggermont, J. J., & Don, M. (1980). Analysis of the click-evoked brainstem potentials in humans using high-pass noise masking. II. Effect of click intensity. *The Journal of the Acoustical Society of America*, 68(6), 1671–1675. <http://doi.org/10.1121/1.385199>

Elberling, C. (1999). Loudness scaling revisited. *Journal of the American Academy of Audiology*, 10(5), 248–260.

Elberling, C., Callø, J., & Don, M. (2010). Evaluating auditory brainstem responses to different chirp stimuli at three levels of stimulation. *The Journal of the Acoustical Society of America*, 128(1), 215–223. <http://doi.org/10.1121/1.3397640>

Elberling, C., & Don, M. (2008). Auditory brainstem responses to a chirp stimulus designed from derived-band latencies in normal-hearing subjects. *The Journal of the Acoustical Society of America*, 124(5), 3022–3037. <http://doi.org/10.1121/1.2990709>

Elberling, C., & Don, M. (2010). A direct approach for the design of chirp stimuli used for the recording of auditory brainstem responses. *The Journal of the Acoustical Society of America*, 128(5), 2955–2964. <http://doi.org/10.1121/1.3489111>

Elberling, C., Don, M., Cebulla, M., & Stürzebecher, E. (2007). Auditory steady-state responses to chirp stimuli based on cochlear traveling wave delay. *The Journal of the Acoustical Society of America*, 122(5), 2772–2785. <http://doi.org/10.1121/1.2783985>

Elberling, C., & Wahlgreen, O. (1985). Estimation of auditory brainstem response, ABR, by means of Bayesian inference. *Scandinavian Audiology*, 14(2), 89–96. <http://doi.org/10.3109/01050398509045928>

Epstein, M., & Silva, I. (2009). Analysis of parameters for the estimation of loudness from tone-burst otoacoustic emissions. *The Journal of the Acoustical Society of America*, 125(6), 3855–3864. <http://doi.org/10.1121/1.3106531>

Fedtke, T., & Hensel, J. (2010). Specification and calibration of acoustic short-term stimuli for objective audiometry, (August), 1–5.

- Fedtke, T., & Richter, U. (2007). Reference zero for the calibration of air-conduction audiometric equipment using “tone bursts” as test signals. *International Journal of Audiology*, 46(1), 1–10. <http://doi.org/10.1080/14992020601050361>
- Ferm, I., Lightfoot, G., & Stevens, J. (2013). Comparison of ABR response amplitude, test time, and estimation of hearing threshold using frequency specific chirp and tone pip stimuli in newborns. *International Journal of Audiology*, 52(6), 419–23. <http://doi.org/10.3109/14992027.2013.769280>
- Florentine, M., & Epstein, M. (2006). TO HONOR STEVENS AND REPEAL HIS LAW (FOR THE AUDITORY STSTEM). *Proceedings of Fechner Day*, 22(1), 37-42.
- Fobel, O., & Dau, T. (2004). Searching for the optimal stimulus eliciting auditory brainstem responses in humans. *The Journal of the Acoustical Society of America*, 116(4 Pt 1), 2213–2222. <http://doi.org/10.1121/1.1787523>
- Gallégo, S., Garnier, S., Micheyl, C., Truy, E., Morgon, a, & Collet, L. (1999). Loudness growth functions and EABR characteristics in Digisonic cochlear implantees. *Acta Oto-Laryngologica*, 119(2), 234–238. <http://doi.org/10.1080/00016489950181738>
- Gallego, S., Micheyl, C., Berger-Vachon, C., Truy, E., Morgon, a, & Collet, L. (1996). Ipsilateral ABR with cochlear implant. *Acta Oto-Laryngologica*, 116(2), 228–233. <http://doi.org/10.3109/00016489609137830>
- Gorga, M. P., Kaminski, J. R., Beauchaine, K. A., & Jesteadt, W. (1988). Auditory brainstem responses to tone bursts in normally hearing subjects. *Journal of Speech and Hearing Research*, 31(1), 87–97.
- Gøtsche-Rasmussen, K., Poulsen, T., & Elberling, C. (2012). Reference hearing threshold levels for chirp signals delivered by an ER-3A insert earphone. *International Journal of Audiology*, 51(11), 794–799. <http://doi.org/10.3109/14992027.2012.705901>
- Greenwood, D. D. (1990). A cochlear frequency-position function for several species--29 years later. *The Journal of the Acoustical Society of America*, 87(6), 2592–2605. <http://doi.org/10.1121/1.399052>
- Hudspeth, a J. (2014). Integrating the active process of hair cells with cochlear function. *Nature Reviews. Neuroscience*, 15(9), 600–614. <http://doi.org/10.1038/nrn3786>
- Hudspeth, a. J. (2008). Making an Effort to Listen: Mechanical Amplification in the Ear. *Neuron*, 59(4), 530–545. <http://doi.org/10.1016/j.neuron.2008.07.012>
- Jewett DL, W. J. (1971). Auditory evoked far-fields averaged from the scalp of humans. *Brain*, (95), 681.
- Jill, C. (2010). Chirp, Chirp.

- Kiessling, J., Schubert, M., & Wagner, I. (1994). Loudness scaling. A procedure for quantitative recruitment detection. *HNO*, *42*(6), 350–357.
- Livro 133 - Auditory evoked potentials.pdf. (n.d.).
- Maloff, E. S., & Hood, L. J. (2014). A Comparison of Auditory Brain Stem Responses Elicited by Click and Chirp Stimuli in Adults With Normal Hearing and Sensory Hearing Loss. *Ear and Hearing*, *35*(2), 271–282. <http://doi.org/10.1097/AUD.0b013e3182a99cf2>
- Marcoux, B. A., & Kurtz, I. (n.d.). Noise Reduction to Achieve Quality ABR Measurement.
- Melcher, J. R. (2009). Auditory Evoked Potentials. *Neuroscience*, *3*(October), 1159–1166. <http://doi.org/10.1016/B978-008043152-9.02245-4>. Author
- Moukos, A., Balatsouras, D. G., & Nikolopoulos, T. (2013). OTOLOGY A longitudinal study of changes in distortion-product otoacoustic emissions and pure-tone thresholds in an industrial setting, 2649–2660. <http://doi.org/10.1007/s00405-013-2754-z>
- Mühler, R., Rahne, T., & Verhey, J. L. (2013). Auditory brainstem responses to broad-band chirps: Amplitude growth functions in sedated and anaesthetised infants. *International Journal of Pediatric Otorhinolaryngology*, *77*(1), 49–53. <http://doi.org/10.1016/j.ijporl.2012.09.028>
- Neely, S. T., Norton, S. J., Gorga, M. P., & Jesteadt, W. (1988). Latency of auditory brain-stem responses and otoacoustic emissions using tone-burst stimuli. *The Journal of the Acoustical Society of America*, *83*(2), 652–656. <http://doi.org/10.1121/1.396542>
- Nolan, K. J., & Parker, D. J. (2000). Use of the 400 Hz period evoked potential in the prediction of loudness discomfort levels in normal hearing adults. *Scandinavian Audiology*, *29*(4), 217–224. <http://doi.org/10.1080/010503900750022844>
- Pickles, J. O. (2012). *July-September 2012 An Introduction to the Physiology of Hearing*.
- Pratt, H., & Sohmer, H. (1977). Correlations between psychophysical magnitude estimates and simultaneously obtained auditory nerve, brain stem and cortical responses to click stimuli in man. *Electroencephalography and Clinical Neurophysiology*, *43*(6), 802–812. [http://doi.org/10.1016/0013-4694\(77\)90003-7](http://doi.org/10.1016/0013-4694(77)90003-7)
- Ribeiro, G., Rodrigues, I., & Lewis, D. R. (2012). Comparison of click and CE-chirp ® stimuli on Brainstem Auditory Evoked Potential recording Potencial Evocado Auditivo de Tronco Encefálico, *17*(2), 412–416.
- Ricketts, T. a., & Bentler, R. a. (1996). The effect of test signal type and bandwidth on the categorical scaling of loudness. *The Journal of the Acoustical Society of America*, *99*(4 Pt 1), 2281–2287. <http://doi.org/10.1121/1.415415>

Robles, L., & Ruggero, M. a. (2001). Mechanics of the mammalian cochlea. *Physiological Reviews*, 81(3), 1305–1352.

Rodrigues, G. R. I., Ramos, N., & Lewis, D. R. (2013). Comparing auditory brainstem responses (ABRs) to toneburst and narrow band CE-chirp® in young infants. *International Journal of Pediatric Otorhinolaryngology*, 77(9), 1555–1560.
<http://doi.org/10.1016/j.ijporl.2013.07.003>

Ruggero, M. a, & Rich, N. C. (1991). Application of a commercially-manufactured Doppler-shift laser velocimeter to the measurement of basilar-membrane vibration. *Hearing Research*, 51(2), 215–230. [http://doi.org/10.1016/0378-5955\(91\)90038-B](http://doi.org/10.1016/0378-5955(91)90038-B)

Ruggero, M. a., & Temchin, A. N. (2007). Similarity of traveling-wave delays in the hearing organs of humans and other tetrapods. *JARO - Journal of the Association for Research in Otolaryngology*, 8(2), 153–166. <http://doi.org/10.1007/s10162-007-0081-z>

Sanchez, J. T., & Gans, D. (2006). Effects of artifact rejection and Bayesian weighting on the auditory brainstem response during quiet and active behavioral conditions. *American Journal of Audiology*, 15(2), 154–163. [http://doi.org/10.1044/1059-0889\(2006\)019](http://doi.org/10.1044/1059-0889(2006)019)

Schnupp, J., Nelken, I., & King, A. (2011). Auditory Neuroscience : Making Sense of Sound, 347.

Serpanos, Y. C., O'Malley, H., & Gravel, J. S. (1997). The Relationship between Loudness Intensity Functions and the Click-ABR Wave V Latency. *Ear & Hearing*, 18(5), 409–419. <http://doi.org/10.1097/00003446-199710000-00006>

Shera, C. a, & Guinan, J. J. (2000). Frequency Dependence of Stimulus-Frequency-Emission Phase: Implications for Cochlear Mechanics. *Recent Developments in Auditory Mechanics Proceedings of the International Symposium*, (July), 381–387.
http://doi.org/10.1142/9789812793980_0054

Silva, I. (2009). Estimation of postaverage SNR from evoked responses under nonstationary noise. *IEEE Transactions on Bio-Medical Engineering*, 56(8), 2123–2130.
<http://doi.org/10.1109/TBME.2009.2021400>

Silva, I., & Epstein, M. (2010). Estimating loudness growth from tone-burst evoked responses. *The Journal of the Acoustical Society of America*, 127(6), 3629–3642.
<http://doi.org/10.1121/1.3397457>

Silva, I., & Epstein, M. (2012). Objective estimation of loudness growth in hearing-impaired listeners. *The Journal of the Acoustical Society of America*, 131(1), 353.
<http://doi.org/10.1121/1.3666024>

Smeds, K., & Leijon, A. (2011). *Loudness* (Vol. 37). <http://doi.org/10.1007/978-1-4419-6712-1>

- Soares, M., Nakazawa, M., Ishikawa, K., Sato, T., & Honda, K. (2014). Hearing screening for Japanese children and young adults using the automated auditory brainstem response. *Auris Nasus Larynx*, *41*(1), 17–21. <http://doi.org/10.1016/j.anl.2013.08.001>
- Stapells, D. R., Galambos, R., Costello, J. a., & Makeig, S. (1988). Inconsistency of auditory middle latency and steady-state responses in infants. *Electroencephalography and Clinical Neurophysiology*, *71*(4), 289–295. <http://doi.org/10.1121/1.2023822>
- Stapells, D. R., Linden, D., Suffield, J. B., Hamel, G., & Picton, T. W. (1984). Human auditory steady state potentials. *Ear and Hearing*, *5*(2), 105–113. <http://doi.org/10.1097/00003446-198403000-00009>
- Stevens, S. S. (1955). The Measurement of Loudness, 471(1921).
- Stevens, S. S. (1957). Concerning the Form of the Loudness Function. *The Journal of the Acoustical Society of America*, *29*(5), 603. <http://doi.org/10.1121/1.1908979>
- Stevens, S. S. (1972). Perceived Level of Noise by Mark VII and Decibels (E). *The Journal of the Acoustical Society of America*, *51*(2B), 575. <http://doi.org/10.1121/1.1912880>
- Stuart, A., & Cobb, K. M. (2014). Effect of Stimulus and Number of Sweeps on the Neonate Auditory Brainstem Response. *Ear and Hearing*, 1–4. <http://doi.org/10.1097/AUD>.
- Stürzebecher, E., Cebulla, M., Elberling, C., & Berger, T. (2006). New efficient stimuli for evoking frequency-specific auditory steady-state responses. *Journal of the American Academy of Audiology*, *17*(6), 448–461. <http://doi.org/10.3766/jaaa.17.6.6>
- Von Békésy, G. (1990). Experiments in Hearing. *The Journal of the Acoustical Society of America*, *88*(6), 2905. <http://doi.org/10.1121/1.399656>
- Wegner, O., & Dau, T. (2002). Frequency specificity of chirp-evoked auditory brainstem responses. *The Journal of the Acoustical Society of America*, *111*(3), 1318–1329. <http://doi.org/10.1121/1.1433805>
- Wilson, K. G., & Stelmack, R. M. (1982). Power functions of loudness magnitude estimations and auditory brainstem evoked responses. *Perception & Psychophysics*, *31*(6), 561–565. <http://doi.org/10.3758/BF03204188>
- Xu, Z. M., Cheng, W. X., & Yao, Z. H. (2014). Prediction of frequency-specific hearing threshold using chirp auditory brainstem response in infants with hearing losses. *International Journal of Pediatric Otorhinolaryngology*, *78*(5), 812–816. <http://doi.org/10.1016/j.ijporl.2014.02.020>
- Yates, G. K., Winter, I. M., & Robertson, D. (1990). Basilar membrane nonlinearity determines auditory nerve rate-intensity functions and cochlear dynamic range. *Hearing Research*, *45*(3), 203–219. [http://doi.org/10.1016/0378-5955\(90\)90121-5](http://doi.org/10.1016/0378-5955(90)90121-5)

M.Sc. Thesis – S. Hoseingholizade; McMaster University – Psychology, Neuroscience and Behaviour.

Yost, W. A. (2013). *Fundamentals of Hearing: An Introduction*. <http://doi.org/9789004236387>

Zhang, J., & Mao, D. X. (2010). Dependence of binaural loudness summation on interaural level difference and frequency for pure tones. *Science China: Physics, Mechanics and Astronomy*, 53(5), 834–841. <http://doi.org/10.1007/s11433-010-0189-8>

Zirn, S., Louza, J., Reiman, V., Wittlinger, N., Hempel, J. M., & Schuster, M. (2014). Comparison between ABR with click and narrow band chirp stimuli in children. *International Journal of Pediatric Otorhinolaryngology*, 78(8), 1352–1355. <http://doi.org/10.1016/j.ijporl.2014.05.028>

Appendix (Matlab Code):

```
% EEGLAB
%loading Data to EEGLAB and do the preprocessing

x=(EEG.data);
x=double(x);
%%% filtering
% All frequency values are in Hz.
Fs = 20000; % Sampling Frequency
Fnotch = 60; % Notch Frequency
BW = 10; % Bandwidth
Apass = 1; % Bandwidth Attenuation
[b, a] = iirnotch(Fnotch/(Fs/2), BW/(Fs/2), Apass);
x_n = filter(b,a,x);

Fstop1 = 50; % First Stopband Frequency
Fpass1 = 100; % First Passband Frequency
Fpass2 = 2000; % Second Passband Frequency
Fstop2 = 4000; % Second Stopband Frequency
Astop1 = 12; % First Stopband Attenuation (dB)
Apass = 1; % Passband Ripple (dB)
Astop2 = 12; % Second Stopband Attenuation (dB)
match = 'passband'; % Band to match exactly

% Construct an FDESIGN object and call its BUTTER method.
h = fdesign.bandpass(Fstop1, Fpass1, Fpass2, Fstop2, Astop1, Apass,Astop2,
Fs);
Hd = design(h, 'butter', 'MatchExactly', match);
y = filtfilt(Hd.sosMatrix,Hd.ScaleValues,x_n);
y=single(y);
EEG.data=y;

%%%%%%%%%%%%%% epoch
EEG = pop_epoch( EEG, { '1' '2' '3' '4' '5' '6' '7' '21' '22' '23'
'24' '25' '26' '27' }, [0 0.05], 'newname', 'CNT file epochs',
'epochinfo', 'yes'); EEG = eeg_checkset( EEG );
% EEG = pop_rmbase( EEG, [-10 0]); EEG = eeg_checkset( EEG );
% number of trials
t=[];
Value=[];
sumEp=1;
t=1;
k=EEG.epoch;
Epvalue = getfield(k(1,1), 'eventtype');
NumEp(1,1)=Epvalue{1}; % trigger name

for i=2: length(k)
% for i=2:4000
Epvalue = getfield(k(1,i), 'eventtype');
NumEp(i)=Epvalue{1};

if NumEp(i)==NumEp(i-1) | NumEp(i)==NumEp(i-1)+20 | NumEp(i)==NumEp(i-1)-
20
sumEp=sumEp+1;

```

```

else
    Value(t,1)=sumEp;
    Value(t,2)= NumEp(i-1);
    sumEp=1;
    t=t+1;
end
end

Value(t,1)=sumEp;
Value(t,2)= Epvalue{1};
%%% seprate trials for averaging
data=EEG.data;
data=squeeze(data);
% data=double(data);
jj=1;
Value(jj,3)=Value(jj,1);
for jj=2:7
    Value(jj,3)=Value(jj,1)+Value(jj-1,3);
end

datacell=cell(1,t); %%% epoched data ; each trigger in each cell

for i=1:7
    a1=Value(i,2);
    b1=mod(a1, 10);
    if i==1
        datacell{1,b1}=data(:,1:Value(i,3));
    else
        datacell{1,b1}=data(:,Value(i-1,3)+1:Value(i,3));
    end
end

%%eliminate DC componant
for j=1:t
    X=datacell{j};
    [Nx,Mx]=size(X);
    X=X-repmat(mean(X),[Nx 1]);
    datacell{j}=X;
end
%%%% artifact rejection
Thr=50; % Threshold
for j=1:t
    X=datacell{j};
    amp=max(abs(X(1:end,:)));
    Thr_ind=find(amp>Thr); %% Thr= threshold
    X(:,Thr_ind)=[]; %% eliminate the trail
    datacell{j}=X;
end

```

```

% main code for doing weighted averaging
%%%initialization
L=8; % number of fixed points
Ep_blcks=10; % number of trials in each block
p=0.001;
%
t=7;
WAV=cell(1,t);
Cn_F=cell(1,t);
Var=cell(1,t);

for j=1:t
    data=datacell{j};
    [vns,data1,blcks]=myAVE(data,L, Ep_blcks);
    [vnsNew]= Ftest(p, vns, L, Ep_blcks);
    VaR{j}=vnsNew; %%% variance of each level
    %%% weighted averaging
    [Cn, Final_WSum]= Weighted_AVE (data1,vnsNew,Ep_blcks,blcks);
    WAV{j}=Final_WSum;
    Cn_F{j}=Cn;
end

%%%%%%%%%%%%%%%%%%%%%%%%%%%%%%%%%%%%%%%%%%%%%%%%%%%%%%%%%%%%%%%%%%%%%%%%mean Vns for each level=W for cftool
meanW=[];
for ii=1:7
    V1=VaR{1,ii};
    k=1;
    T=[]; B=[];
    a1=V1(1,1);
    B(k,1)=a1;

    for i=1:length(V1)
        if V1(i,1)~=a1
            T(k,1)=i-1;
            B(k,1)=V1(i-1,1);
            k=k+1;
            a1=V1(i,1);
        end
    end
end

if T(k-1,1)~=length(V1)
    T(k,1)=length(V1);
    B(k,1)=V1(length(V1),1);
end

T(1,2)=T(1,1);
for i=2:length(T)
    T(i,2)=T(i,1)-T(i-1,1);
end
Temp_W=sum(T(:,2).*B(:,1))/(length(V1)^2);
meanW(1,ii)=Temp_W;
V1=[];
end
W_final=1./meanW;

```

% function to calculate the variances

```
function [vns,data1,blcks]=myAVE(data, L, Ep_blcks)

[N M]=size(data); % N= data length M=number of trials
delta= ceil(N/L); % delta= distance among L multiple fixed point
blcks= floor(M/Ep_blcks); % number of blocks; within each block there are
Ep_blcks trials.
a=mod(M,blcks);
data1=data(:,1:end-a);

Newdata=data1(1:delta:end,:);
Ave_data=reshape(Newdata,[L,Ep_blcks,blcks]);
Var_data=var(Ave_data,0,2);
vns=mean(Var_data);
vns=squeeze(vns); %%%Remove singleton dimensions
end
```

% function to do the F-test to determine the independent noise sources

```
function [vnsNew]= Ftest (p, vns, L, Ep_blcks)
k=1;
TEMPT=vns;
for m=1:length(TEMPT)-1
    V1= TEMPT(m,1);
    V2=TEMPT(m+1,1);
    F=V1/V2;
    d2=L*Ep_blcks-1;
    d1=L*k*Ep_blcks-1;
    F05=finv(p,d1,d2);
    F95=finv(1-p,d1,d2);
    if ( F >= F05 && F <= F95)
        Q=k*Ep_blcks/Ep_blcks;
        Vnew= (Q*V1+V2)/(Q+1);
        TEMPT(m-k+1:m+1)=Vnew;
        k=k+1;
    else
        k=1;
    end
end
vnsNew=TEMPT;
end
```

% function to do the weighted averaging

%%% weighted averaging

```
function [Cn, Final_WSum]= Weighted_AVE (data1,vnsNew,Ep_blcks,blcks)
S1=[]; Data=[];
[N M]=size(data1);
for i=1:blcks
    Data_vns(:,1+Ep_blcks*(i-1):Ep_blcks*i)=repmat(vnsNew(i,1),N,Ep_blcks);
end
Cn1=1./Data_vns;
Cn=sum(Cn1(1,:));
S1=data1./Data_vns;
Sum_sig=sum(S1,2);
Final_WSum=Sum_sig./Cn;

end
```

% function to do the normal averaging

%%% Normal averaging

```
function [Final_NSum]= Normal_AVE (data)
Sum_sig2(:,1)=sum(data,2);
[N M]=size(data);
Final_NSum= Sum_sig2.*1/M;

end
```